Bulletin of the Seismological Society of America, Vol. 96, No. 1, pp. 107–132, February 2006, doi: 10.1785/0120040231

Layered Seismogenic Source Model and Probabilistic Seismic-Hazard Analyses in Central Italy

by Bruno Pace, Laura Peruzza, Giusy Lavecchia, and Paolo Boncio

Abstract We defined a seismogenic model for central Italy based on three layers of sources and computed the relative seismic-hazard maps. One layer is constituted by individual structures liable to generate major earthquakes ($M \geq 5.5$). We defined them as seismogenic boxes by using geological information in terms of plan projection of active faults; the seismicity rates associated with an individual source are based on the geometry and kinematics of the fault; the recurrence model is controlled by the earthquake-source association, and, when possible, we defined the occurrence time of the last major event, using it in a time-dependent approach. Another layer is given by the instrumental seismicity analysis of the past two decades, which allows us to evaluate the background seismicity ($M \sim< 5.5$); using a sliding-window selection of events, we defined a model of regular adjacent cells of variable *a* and *b* values of the Gutenberg-Richter relation. The last layer utilizes all the instrumental earthquakes and the historical events not correlated to known structures ($4.5 < M \sim< 6$), by separating them into seismotectonic provinces shaped on a geological-structural basis. The seismic-hazard computations first use this layered model in a traditional probabilistic scheme. The results indicate a narrow belt of peak ground acceleration (PGA) higher than 0.30*g* (with standard deviation in attenuation functions) in the axial part of the Apennine chain, with a maximum spot of PGA >0.40*g* southeast of the area damaged by the 1997–1998 Umbria-Marche sequence (PGA expected not to be exceeded in 50 years at 90% probability level). The background seismicity gives a nonnegligible contribution to the hazard, at least for first damage levels. Then, a simplified time-dependent hypothesis has been introduced for the individual sources alone, computing the conditional probability of occurrence of characteristic earthquakes for each source by Brownian passage time distributions. Adopting equivalent fictitious seismicity rates, we obtained maps referring to the next 50 years by using traditional codes. These results show that the contribution of the recently active sources vanishes, and the most hazardous sites are now located south of L'Aquila and in the Sulmona area. We consider that the methodology and results obtained are useful for seismic risk reduction strategies.

Introduction

In recent years, the integration of geological, seismological, and geophysical information has led to a much better, though still far from complete, understanding of the relationships between faults and earthquakes in space and time, with major advances in the science of probabilistic seismic hazard (PSH) analysis. In particular, some efforts have been focused toward developing multidisciplinary PSH models that combine geological data (fault length, slip rate, and paleoearthquake data) with historical seismicity data to estimate the future ground motion (WGCEP, 1995, 1999, 2003; Stirling *et al.*, 2002; Frankel *et al.*, 2002; Field *et al.*, 2003). The use of geological inputs is useful in cases of incomplete historical records and in areas of diffuse deformation or slowly interacting plate boundaries, where large earthquakes may recur every 10^3–10^5 years. In these cases, traditional seismotectonic zoning, based primarily on earthquake frequency statistics obtained from historical catalogs of seismicity and conventional seismic hazard assessments, can be inadequate, even while remaining the standard, basic analyses for seismic zonation purposes.

Long recurrence times for the largest events and diffuse deformation are common in Italy. Some seismogenic sources have slip rates lower than 1 mm/yr and recurrence times for surface-faulting events comparable to or longer than the completeness interval of the historical information (e.g., 800–1000 years in the central Apennines according to Stucchi and Albini, 2000); seismotectonic and paleoseismological studies (e.g., Galadini and Galli, 2000; Morewood and Roberts, 2000; Valensise and Pantosti, 2001; Boncio *et al.*, 2004a) have confirmed that some sources have been silent in the historical catalog time window, but active in the Late Quaternary. In recent years, these studies have changed the common thinking that the Italian earthquake catalogs are long enough and complete enough to estimate all the seismicity levels. In Italy, the PSH analyses developed for seismic zonation purposes use basically an earthquake statistics linked to seismotectonic zoning and historical catalogs (see Slejko *et al.*, 1998; Meletti *et al.*, 2000; Scandone and Stucchi, 2000; Gruppo di Lavoro, 1999, 2004; Romeo *et al.*, 2000; Albarello *et al.*, 2000; Lucantoni *et al.*, 2001); only some authors have introduced cautious statistical criteria concerning the maximum magnitudes (e.g., Slejko *et al.*, 1998; Gruppo di Lavoro, 2004), but no one has explored the computation geometries and/or seismicity rates derived directly from geological and paleoseismological observations. Nevertheless, the occurrence in 1997–1998 of the Umbria-Marche earthquake sequence signaled a turning point in the development of new models and methods for Italian PSH studies. Models aiming to define individual sources (seismogenic structures) responsible for major earthquakes, which can be supported by detailed geological evidence, give an independent constraint to the characterization of the seismicity (Barchi *et al.*, 2000; Galadini and Galli, 2000; Galadini *et al.*, 2000; Valensise and Pantosti, 2001; Boncio *et al.*, 2004a). By addressing individual sources, the methods could enhance the introduction of time-dependent issues and some attempts to apply these approaches have already been published (e.g., Peruzza *et al.*, 1997; Faenza *et al.*, 2003; Marzocchi *et al.*, 2003; Romeo, 2005).

The central Apennines are the best known area in Italy where such analyses can be performed. Following some preliminary studies (Peruzza, 1999; Peruzza and Pace, 2002; Pace *et al.*, 2002b; Boncio *et al.*, 2004a) that exclusively use individual sources to define the expected seismicity and introduce time-dependent assumptions, in this article we propose a new, more complex and complete seismogenic source model for central Italy. It is based on three combined layers of information to compute the relative seismic-hazard maps under Poisson and non-Poisson hypotheses.

Seismotectonic Context

In this section, we briefly describe the active tectonic setting of central Italy (Fig. 1), an area where many detailed surface and deep geological/geophysical data, and good records of paleo- and historical earthquakes are available. In the following text we apply the term seismotectonic provinces (SPs) to large structural domains, homogeneous in terms of active tectonics. Within the provinces we identify, whenever possible, seismogenic boxes (SBs), which are the map projection of individual active faults responsible for or capable of experiencing major earthquakes ($M \geq 5.5$). We consider active the faults that show clear geological evidence of repeated displacement episodes during Late Quaternary (i.e., the last 125 kyr) and/or clear association with paleoearthquakes (recognized in trenches), historical earthquakes (reported in earthquake catalogs), and recent seismic sequences (recorded instrumentally).

In Figure 1, we plotted some main tectonic elements and selected focal mechanisms. Note that all the recognized individual active faults are located along the Apennine chain (Boncio *et al.*, 2004a).

The Seismotectonic Provinces

The nature and distribution of the seismicity and of the active structures indicate that the active deformation field of central Italy is mainly characterized by extension in the axial zone of the Apennines and by contraction in the frontal part of the belt, close to the Adriatic sea border (Lavecchia *et al.*, 1994, 2002, 2003; Frepoli and Amato, 1997; Montone *et al.*, 1999). From the Tyrrhenian coast to the Adriatic coast, we identify four SPs parallel to the Apennines (Fig. 2): A, the Tuscan-Latium SP; B, the Apennine SP; C, the foothill SP; and D, the coastal-Adriatic SP. To define the boundaries between the provinces, we mainly take into account the 3D geometry of major active structural elements, together with seismological data such as earthquake focal mechanisms, rheologic and geodetic data. Our description, in geological terms, of the provinces follows.

SP A. The Tuscan-Latium thinned crust SP is a structural domain that underwent Neogene extensional tectonics, with northwest–southeast trending extensional basins mainly of the Late Miocene-Pliocene (Decandia *et al.*, 1998). Regional uplift affected the area, mainly during the Late Pliocene and after 1 Ma hence (Argnani *et al.*, 1997, 2003). Presently, it is characterized by a thin crust (average, 22 km), high heat-flow values, and positive gravimetric anomalies. The active deformation field mainly consists of subordinate vertical tectonics because of isostatic rebound processes and localized zones of deformation corresponding to Quaternary volcanoes and/or geothermal areas (e.g., Larderello-M. Amiata geothermal areas in Tuscany, Volsini Mountains volcanic complex in northern Latium, and Colli Albani volcanic complex southeast of Rome; Fig. 1). On average, the seismic activity is small ($M < 5.5$) and located within the upper crust, mostly at depths shallower than 7 km (Amato *et al.*, 1998; Working Group Catalogo Parametrico dei Terremoti Italiani [CPTI], 2004; Working Group Catalogo Strumentale dei Terremoti Italiani [CSTI], 2001). The earthquake focal mechanisms and borehole breakout data indicate a prevailing extensional regime (see Fig. 1) (Frepoli and Amato, 1997; Montone *et al.*, 1999).

SP B. The Apennine extensional SP is a structural domain that has undergone southwest–northeast extension since the

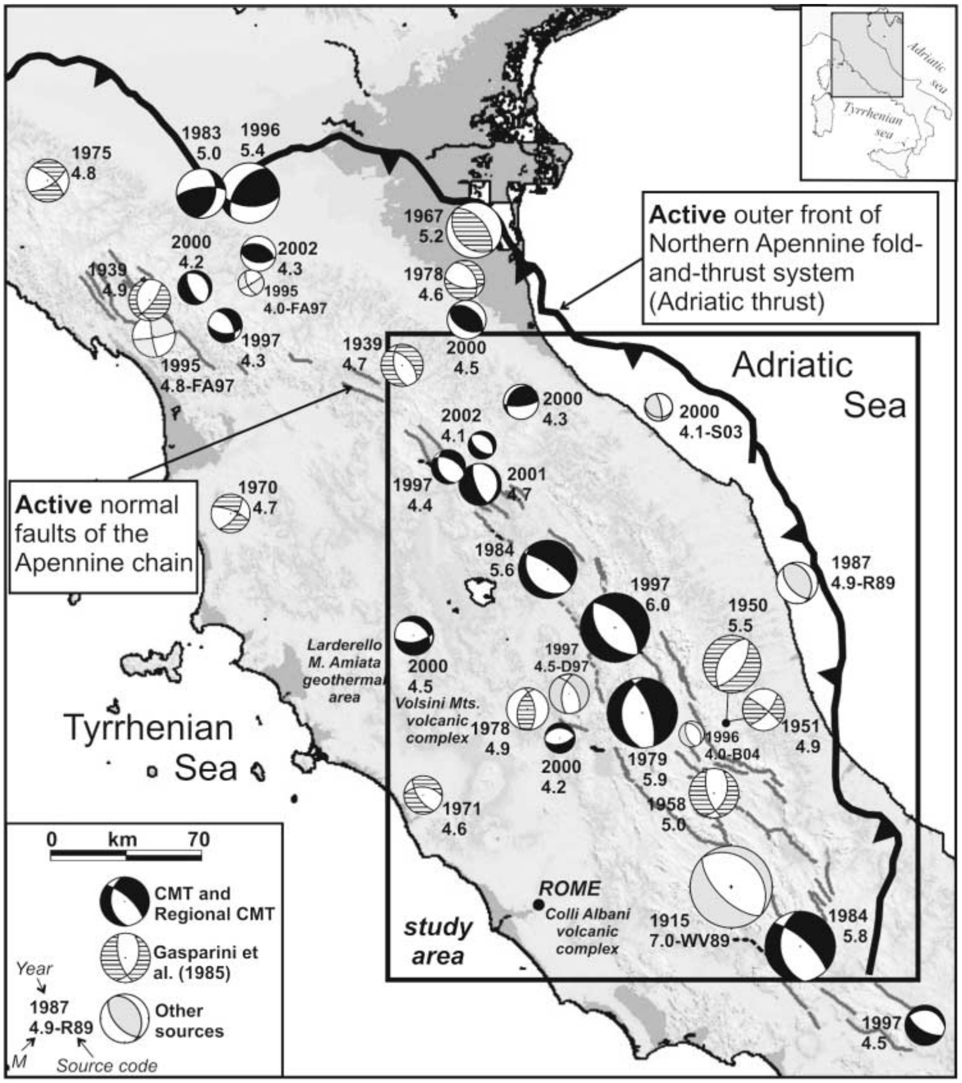

Figure 1. Shaded relief of central Italy with tectonic elements and focal mechanisms. Selected earthquakes with $M \geq 4.0$ from 1915 to 2002 (from Montone *et al.*, 1999, implemented). Black focal mechanisms taken from Harvard centroid moment tensor (CMT) catalog at www.seismology.harvard.edu and MedNet regional CMT at www.mednet.ingv.it. The source codes are as follows: R89, Riguzzi *et al.* (1989); WV89, Ward and Valensise (1989); FA97, Frepoli and Amato (1997); D97, Di Luccio *et al.* (1997); S03, Santini (2003); B04, Boncio *et al.* (2004b).

Middle Pliocene. It is presently characterized by active northeast- and southwest-dipping normal and normal-oblique faults, mainly located along the axial belt of the Apennines, with associated intramontane basins. The active extensional regime is constrained by numerous earthquake focal mechanisms, Quaternary fault-slip data, and related stress analysis (e.g., Frepoli and Amato, 1997; Montone *et al.*, 1999; Boncio and Lavecchia, 2000a; Boncio *et al.*, 2004a), geodetic data (Hunstad *et al.*, 2003), and morphotectonic and paleoseismological data (e.g., Blumetti, 1995; Michetti *et al.*, 1996; Pantosti *et al.*, 1996; Galadini and Galli, 2000; D'Addezio *et al.*, 2001). Relatively frequent and moderate magnitude earthquakes ($4.0 < M \leq 6.0$) recorded instrumentally over the past 20 years (see Figs. 1 and 2), as well as large historical earthquakes (macroseismic intensity up to XI on the Mercalli Cancani Sieberg (MCS) scale, M up to 7.0; see Fig. 3) with long recurrence intervals occur in this province. They are mainly concentrated in the upper crust, at depths $\leq$15 km (Boncio *et al.*, 2004a).

The western boundary of the province (between SP A and B in Fig. 2) has different geological constraints along its length; in the northern part (the a–b segment in Fig. 2), the boundary coincides with the surface trace of an active regional-scale east-dipping low-angle extensional detachment fault, named Etrurian Fault System (EFS) (see Boncio *et al.*, 2000; Lavecchia *et al.*, 2002, for details). The EFS

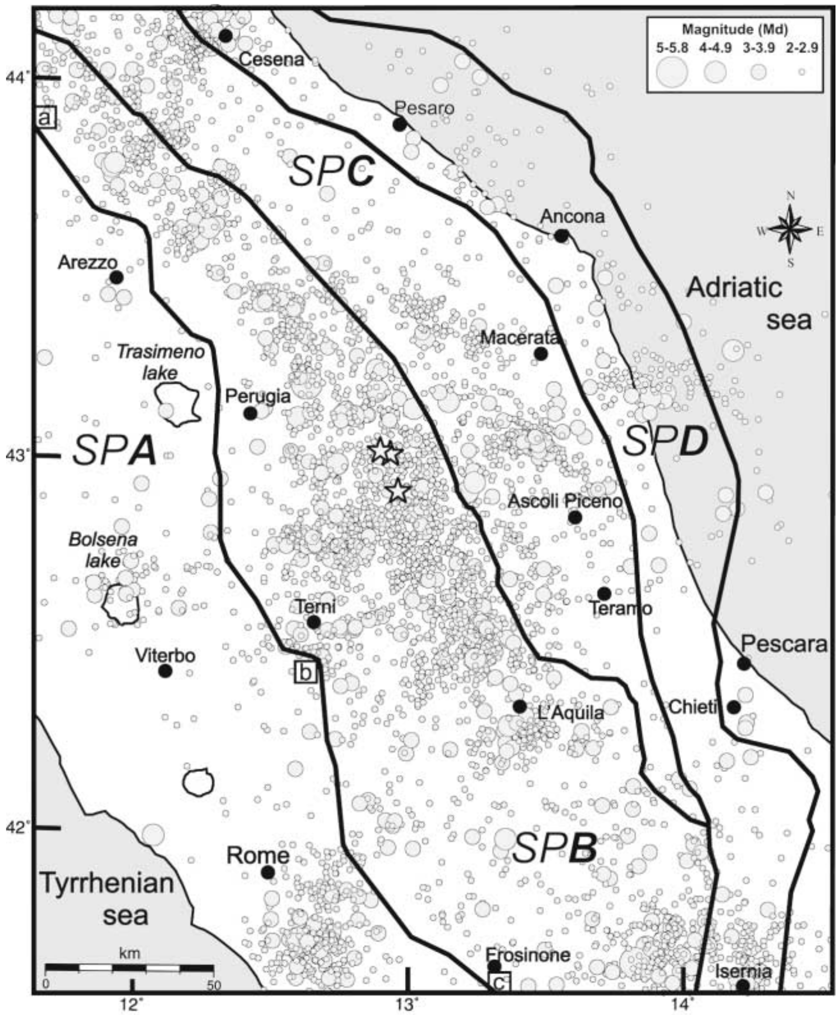

Figure 2. Map of the seismotectonic provinces (SPs) of central Italy and epicenters of instrumental earthquakes recorded in the period 1981–1996 (data from CSTI catalog, Working Group CSTI [2001], after removal of aftershocks as explained in the text). The epicenters of the mainshocks of the 1997–1998 Umbria-Marche seismic crisis (26 September 1997 00:33, M_w 5.7; 26 September 1997 09:40, M_w 6.0; 14 October 1997 M_w 5.6; Amato *et al.*, 1998) are plotted with stars.

controls the active extension and seismicity of SP B in the northern Apennines. In the southern part (the b–c segment in Fig. 2), the boundary is less constrained because no data confirm the presence of the EFS; it has been placed along the western border of the high topographic range of the Apennines, where the major extensional processes occur.

The eastern boundary of the SP B represents the eastern border of the crust, which is clearly undergoing extension, on the basis of all the available geological (surface and subsurface), seismological and geodetic data.

SP C. The foothill SP corresponds to an area situated in an intermediate position between the Apennines, undergoing extension, and the coastal-Adriatic zone, undergoing contraction. Both shallow (<15 km) and relatively deep (15–25 km) small-magnitude earthquakes have been recorded recently (Parolai *et al.*, 2001; Lavecchia *et al.*, 2003). Some of the historical earthquakes with MCS intensities up to IX–X (*M* up to 6.2; Fig. 3) occurred in the province, especially in the western part. The few available focal mechanisms are of mixed kinematics, with either normal, strike-slip, or reverse-faulting mechanisms, suggesting that the tectonic regime is not uniform within the province (Fig. 1) (Gasparini *et al.*, 1985; Frepoli and Amato, 1997; Mednet database at http://mednet.ingv.it, last accessed November 2004). Lavecchia *et al.* (2003) proposed a seismotectonic model with a change of the tectonic regime with depth: the lower crust is considered under contraction and cut by a still active west-dipping crustal thrust (the Adriatic Thrust) which would be seismogenic in the 15–25 km depth interval (upper part of the lower crust) according to the rheological stratification of the crust; the upper crust (depths <15 km) would be mainly under extension. The highly damaging historical earthquakes, with intensities IX–X MCS, such as Offida 1943, Camerino 1799, Fabriano 1741, and Cagli 1781, might be associated with relatively deep (15–25 km) thrust faulting.

SP D. The coastal-Adriatic contractional SP is a structural domain characterized by folds, thrusts, and strike-slip faults nucleated from Middle Pliocene at the hanging-wall of the Adriatic Thrust (Lavecchia *et al.*, 2003). The Adriatic Thrust emerges along the eastward convex Adriatic front and deepens westward; its geometry at depth is constrained by the CROP 03 deep seismic reflection profile (Pialli *et al.*, 1998).

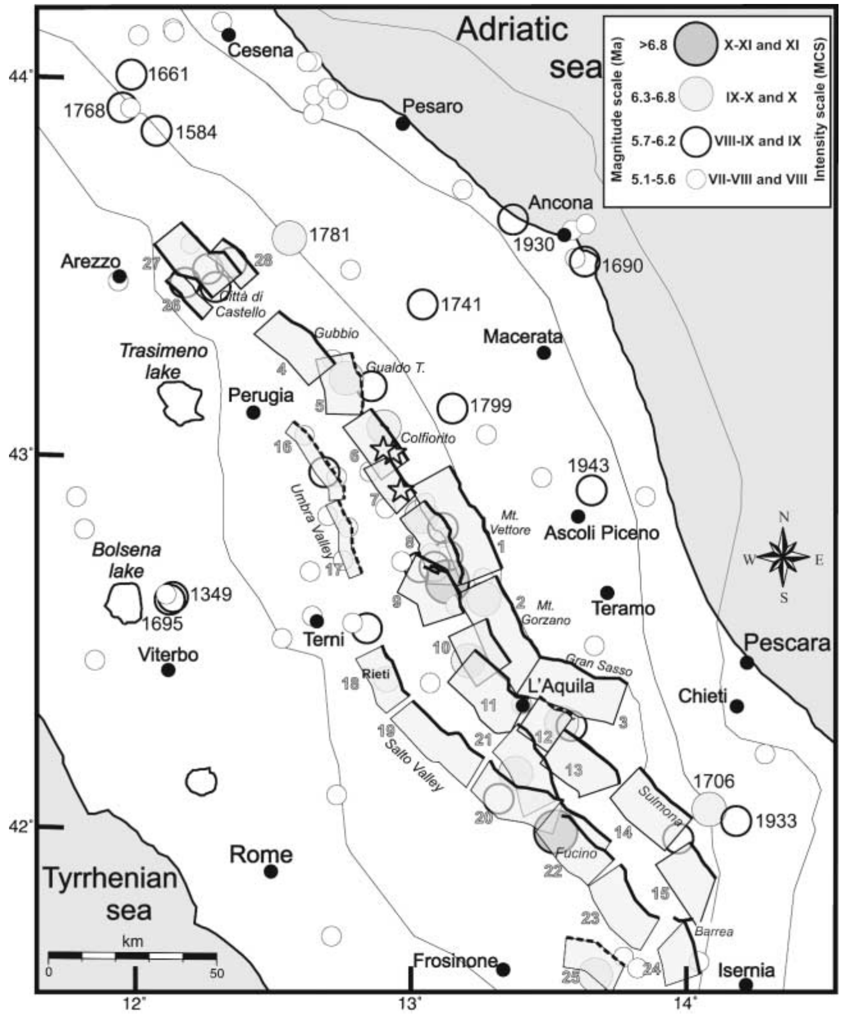

Figure 3. Map of the seismogenic boxes (SBs) of central Italy and epicenters of historical earthquakes with epicentral intensity larger than VII–VIII MCS (corresponding roughly to $M > 5.1$, Working Group CPTI, 2004). The dates refer to the earthquakes outside the SP B with epicentral intensity larger than VIII MCS. The stars are the epicenters of the mainshocks of the 1997–1998 Umbria-Marche seismic crisis (Amato *et al.*, 1998); *SBs* are marked with numbers (see Tables 1 and 2).

The province is characterized by upper crust seismicity (mostly <10 km) never exceeding *M* 5.0 during the past 30 years; examples are the events of Ancona 1972 (M_s 4.5; Gasparini *et al.*, 1985), Porto San Giorgio 1987 (M_d 4.9; Riguzzi *et al.*, 1989), and offshore Pesaro 2000 (*M* 4.1; Santini, 2003), with prevailing thrust and strike-slip focal solutions and *P*-axes trending from southwest–northeast to east–west (Fig. 1). Historical earthquakes, probably of shallow hypocentral source, have intensities up to IX MCS (*M* up to 5.9) but mostly below IX. The eastern boundary of the SP D coincides with the front of the Adriatic thrust. The western boundary (between SP C and D of Fig. 2) corresponds to the surface projection of the intersection line between the Adriatic thrust and the base of the brittle layer, which, in this area, is at ~10 km depth, according to rheological and seismicity data (Lavecchia *et al.*, 2003).

The Seismogenic Boxes

Most of the strong earthquakes of central Italy fall inside SP B, within the Apennine chain. Moreover, only in this sector do the active faults have unequivocal seismogenic characteristics at the surface. Compilations of individual seismogenic sources have been proposed recently for this area (Barchi *et al.*, 2000; Galadini and Galli, 2000; Galadini *et al.*, 2000; Valensise and Pantosti, 2001; Boncio *et al.*, 2004a). In this article, we use the model of 3D seismogenic sources proposed by Boncio *et al.* (2004a), which is based on an interdisciplinary analysis integrating structural-geological (surface and subsurface), morphotectonic, paleoseismological, seismological, and rheological data. It provides the geometry, kinematics, and first-order segmentation pattern of the major active seismogenic faults, liable to undergo large earthquakes ($M \geq 5.5$).

Figure 3 shows the SBs identified in central Italy. The original model by Boncio *et al.* (2004a) has been implemented with the seismogenic sources of the northern part of SP B (SBs 26, 27, and 28), defined on the basis of an original seismotectonic analysis (Brozzetti *et al.*, 2001). Table 1 summarizes the geometrical characteristics of each source, used later on as input parameters for seismic hazard analyses. The maximum rupture area (RA) has been calculated from the along-strike length (L) and the down-dip length (W), assuming a simplified rectangular shape of the source.

Table 1
Geometric Parameters of the Seismogenic Boxes (SB) in Central Italy*

	Seismogenic Boxes	L (km)	D (km)	W (km)	RA (km²)	SR (mm/yr)	References
1	Bove-Vettore	35.0	15.0	19.6	686	0.5	G03a
2	Gorzano	28.4	15.0	19.6	557	0.3	G03a
3	Gran Sasso	28.7	15.0	19.6	563	0.8	G03b; G95
4	Gubbio	23.64 (20.9)	6.0	12.0	251	0.8	B00; V01
5	Gualdo Tadino	19.3	8.0	14.0	270	0.5	B00; V01
6	Colfiorito	19.1	8.5	14.0	267	0.5	B00; V01
7	S. Martino-Civitella	14.2	6.5	10.0	142	0.6	B00; V01
8	Nottoria-Preci	29.0 (27.6)	12.0	15.5	428	0.6	B00; V01
9	Cascia-Cittareale	24.2	13.5	17.6	426	0.6	B00; V01
10	Montereale	16.2	15.0	19.6	318	0.6	B00; V01
11	Pizzoli-Pettino	24.0	15.0	19.6	470	0.6	B00; V01
12	Paganica	13.0	15.0	19.6	255	0.6	B00; V01
13	Media Valle Aterno	24.0	15.0	19.6	470	0.3	B00; V01
14	Sulmona	23.5	15.0	19.6	461	0.5	B00; V01
15	Pizzalto-Cinquemiglia	18.0	15.0	19.6	353	0.4	D01; F89
16	Valle Umbra N	28.7 (9.0)	4.5	5.9	53	0.8	B00; V01
17	Valle Umbra S	23.9 (9.0)	4.5	5.9	53	0.8	B00; V01
18	Rieti	16.5	10.0	13.1	216	0.5	B00; V01
19	Valle del Salto	28.4 (25.4)	11.0	14.4	366	0.5	B00; V01
20	Velino-Magnola	26.5	12.5	16.3	432	0.5	B00; V01
21	Campo Felice-Ovindoli	26.5	13.0	17.0	451	0.8	P96; S03
22	Fucino	25.0	13.0	17.0	425	0.7	G97a; G97b; G99
23	M. Marsicano	21.0	13.0	17.0	357	0.6	B00; V01
24	Barrea	17.4	13.0	17.0	296	0.4	B00; V01
25	Sora	20.0	11.0	14.4	288	0.3	B00; V01
26	M.S. Maria Tiberina	16.0 (10.2)	2.5	6.5	66	0.5	B00; V01
27	Città di Castello	24.5 (15.0)	3.0	9.0	135	0.5	B00; V01
28	Parnacciano	14.0	4.0	9.0	126	0.5	B00; V01

*L, along-strike length, in parentheses corrected values (see the text); D, thickness of the local seismogenic layer; W, down-dip length; RA, maximum rupture area. SR is the slip rate assigned to the sources, using the references available: B00, Barchi *et al.*, 2000; D01, D'Addezio *et al.*, 2001; F89, Frezzotti and Giraudi, 1989; G95, Giraudi and Frezzotti, 1995; G97a, Galadini *et al.*, 1997a; G97b, Galadini *et al.*, 1997b; G99, Galadini and Galli, 1999; G03a, Galadini and Galli, 2003; G03b, Galadini *et al.*, 2003; P96, Pantosti *et al.*, 1996; S03, Salvi *et al.*, 2003; V01, Valensise and Pantosti, 2001.

L represents the length of the major structures (seismogenic master faults) that may be slightly discontinuous at the surface (small-scale segmentation), but it can be considered continuous at depth, as it is not interrupted by first-order (kilometer scale) structural-geometrical complexities. W has been evaluated from the average inclination of the faults and the thickness of the local seismogenic layer.

The SBs are characterized by a set of paleoseismological, historical, and/or instrumental earthquakes. The SB-earthquake associations are given in Table 2, whereas a more general description of the seismological databases is reported in the next section. Paleoevents, when available, are recorded in the table. Historical earthquakes have been associated to the SB by the analysis of the distribution of the highest intensity data points; instrumental earthquakes by seismological considerations, such as the distribution of the aftershock sequences.

In detail, the easternmost boxes (SB 1–3) are characterized by some prehistoric events defined by paleoseismological analyses in trenches, but none of the historical events of the area can be satisfactorily correlated to these structures, except for the 1639 earthquake (I = X, M 6.3) which ruptured the northern portion of SB 2 (M. Gorzano). The intermediate seismogenic boxes (SB 4–15 and 26–28) are the most seismically active; they are characterized by some prehistoric earthquakes (SB 15), and several historical and instrumental earthquakes (for details see Table 2 and Boncio *et al.*, 2004a). The westernmost seismogenic boxes (SB 16–25) are in some places less constrained from geological data, and their seismogenic importance is debated. This is the case of SB 16 and 17, SB 18 (Michetti *et al.*, 1995), and SB 25. In the central-southernmost sector, several paleoseismological (SB 21 and 22), historical (September 1349, February 1904, January 1915, July 1654), and instrumental (May 1984) earthquakes occurred (see Table 2 for associations and references). In some cases (see the examples of SB 1, 8, and 9 or 2, 10, and 11) we have partial overlap of sources, motivated by the 3D fault geometry. The overlaps can have considerable influence on the seismic hazard results, but we currently do not have data to refute the complex 3D geometry.

Outside the SP B we actually have no comparable seismotectonic information. By using fault dimensions that derive from magnitude and constraining the geometrical pat-

Table 2
Earthquake-Source Association Adopted for Seismogenic Boxes in Central Italy*

		Historical Earthquakes† ($I_0 \geq$ VII-VIII MCS)							Instrumental Earthquakes‡ ($M > 4.5$)					
	Seismogenic Boxes	yyyy/mm/dd	I_{max}	I_o	M_s	M_o	M_m	M_a	yyyy/mm/dd	M_s	M_w	M_t	Paleoseismological Earthquakes§	References
1	Bove-Vettore												4155/3965 BP-600/700 AD	
													5940/5780 BP-4155/3965 BP	G03a
													18000/12000 BP-5940/5780 BP	
2	Gorzano	1639/10/07	X	X		5.9	6.6	6.3					after 8320/8150 BP	G03a; B04
													after 8320/8150 BP	
3	Gran Sasso												after 3480/3400 BP	
													7155/7120 BP-7035/6790 BP	G03b; G95
													late Pleistocene	
4	Gubbio	1593/04/23	VII-VIII	VII-VIII		5.6	5.1	5.3	1984/04/29	5.2	5.6	5.2		ISC; Ha; CSI
5	Gualdo Tadino	1747/04/17 (?)	IX	IX		5.9	6.0	5.9	1998/04/03	4.8	5.1	5.3		A98; BL00; C98;
		1751/07/27	X	X		6.2	6.6	6.3						Ca00; Ci00; CSI
6	Colfiorito	1279/04/30	X	X		6.1	6.6	6.3	1997/09/26 00.33	5.5	5.7	5.6		A98; BL00; C98:
									1997/09/26 09:40	5.9	6.0	5.8		Ca00; Ci00; CSI
7	S. Martino-	1791/10/11	VII-VIII	VII-VIII		5.0	5.1	5.0	1997/10/12	4.9	5.2			
	Civitella	1838/02/14 (?)	VIII	VIII		5.7	5.4	5.5	1997/10/14	5.5	5.6			
8	Nottoria-Preci	1328/12/01	X	X		6.2	6.6	6.4	1979/09/19	5.9	5.9			S85; B95; CFTI
		1703/01/14	XI	XI		6.8	7.1	6.8						
		1719/06/27	VII-VIII	VII-VIII		5.0	5.1	5.0						
		1730/05/12	IX	VIII-IX		5.9	5.8	5.8						
		1815/09/03	VII-VIII	VII-VIII			5.1	5.1						
		1859/08/22	VIII-IX	VIII-IX		5.3	5.8	5.6						
9	Cascia-Cittareale	1599/11/05	VIII-IX	VIII-IX		5.7	5.8	5.8						
		1916/11/16		VII-VIII	5.3		5.1	5.3						
10	Montereale	1703/01/16 ($)	VIII	VIII		6.0								S85; B95; CFTI
11	Pizzoli-Pettino	1703/02/02	X	X		6.7	6.6	6.7						S85: B95; CFTI
12	Paganica	1461/11/26	X	X		6.1	6.6	6.5	1958/06/24 (#)	5.0				G85
		1762/10/06	IX-X	IX		5.5	6.0	5.9						
13	Media V. Aterno													
14	Sulmona	100												G01
15	Pizzalto-	1315/12/03	X	IX			6.0	6.0					1349 AD–800 BC	
	Cinquemiglia												3735 BC–2940 BC	D01; F89
													3540 BC–7000 BP	
16	Valle Umbra N	1832/01/13	VIII-IX	VIII-IX		5.6	5.8	5.7						
		1854/02/12	VII-VIII	VII-VIII			5.1	5.1						
17	Valle Umbra S	1745/03	VIII	VII-VIII			5.1	5.1						
		1767/06/05	VII-VIII	VII-VIII		5.3	5.1	5.2						
		1878/09/15	VIII	VIII		5.3	5.4	5.4						
18	Rieti	1298/12/01 (?)	IX-X	VIII-IX		6.2	5.8	5.9						
		1898/06/27	VIII	VII-VIII		5.3	5.1	5.3						
19	Valle del Salto													
20	Velino-Magnola	1904/02/24	IX	VIII-IX	5.5	5.5	5.8	5.5						
21	Campo Felice-	1349/09/09	X	IX-X		7.1	6.3	6.5					1300 AD–1690 BC	
	Ovindoli												1420 BC–5620 BC	P96; S03
													5460 BP–20000 BP	
22	Fucino	1915/01/13	XI	XI	7.0	7.0	7.1	7.0					508 AD–618 AD	
													1100 BC–1600 BC	
													2200 BC–3944 BC	G97a; G97b;
													400 BC–5979 BC	G99
													5979 BC–10729 BC	
													10053 BC–10729 BC	
23	M. Marsicano													
24	Barrea								1984/05/07	5.8	5.9	5.9		P02; CSI
25	Sora	1654/07/23	X	IX-X		6.1	6.3	6.2						
		1922/12/29 (*)	VII	VII	5.5	5.2	4.8	5.4						
26	M.S. Maria	1352/12/25	IX	IX			6.0	6.0						
	Tiberina	1917/04/26	IX-X	IX	5.6	5.9	6.0	5.7						
27	Città di Castello	1458/04/26	IX	IX		5.6	6.0	5.8	2001/11/26		4.7	4.4		CSI
		1789/09/30	IX	VIII-IX		5.6	5.8	5.7						
28	Parnacciano	1389/10/18	IX	IX			6.0	6.0						

(*footnotes on following page*)

†Parameters of historical earthquakes are taken from the CPTI catalog (Working Group CPTI, 2004): magnitude types are quoted in the text (for further details, see at http://emidius.mi.ingv.it/CPTI04/presentazione.html); when not specified (B95, Blumetti, 1995; CFTI, Boschi *et al.*, 1997; S85, Stucchi, 1985), the intensity point distributions derive from Monachesi and Stucchi, 1997.

‡Instrumental earthquake references are: A98, Amato *et al.*, 1998; BL00, Boncio and Lavecchia, 2000b; B04, Boncio *et al.*, 2004b; C98, Cello *et al.*, 1998; Ca00, Cattaneo *et al.*, 2000; Ci00, Cinti *et al.*, 2000; CSI, Castello *et al.*, 2005; G85, Gasparini *et al.*, 1985; Ha, Harvard Catalog at www.seismology.harvard.edu/; ISC, ISC Bulletin at www.isc.ac.uk/Bulletin/rectang.htm; P02, Pace *et al.*, 2002a.

§Date and association of the paleoearthquakes are those suggested by: D01, D'Addezio *et al.*, 2001; F89, Frezzotti and Giraudi, 1989; G95, Giraudi and Frezzotti, 1995; G97a, Galadini *et al.*, 1997a; G97b, Galadini *et al.*, 1997b; G99, Galadini and Galli, 1999; G01, Galadini and Galli, 2001; G03a, Galadini and Galli, 2003; G03b, Galadini *et al.*, 2003; P96, Pantosti *et al.*, 1996; S03, Salvi *et al.*, 2003.

*?, uncertain earthquake-source association; $, earthquake not in the CPTI catalog; #, association from epicenter and relative focal mechanism; *, historical earthquake below the threshold of I_o, but with instrumental magnitude $M_s > 5.5$.

tern by intensity data points of historical earthquakes, some authors (e.g., Gasperini *et al.*, 1999; Valensise and Pantosti, 2001) propose seismogenic boxes whose definition criteria are therefore different from ours; we do not use them for the sake of homogeneity, but let the seismogenic potential of earthquakes belong to the province.

Seismological Databases

Italy has a well-known tradition of earthquake catalogs, starting with the seismological compilations of the beginning of the twentieth century (Baratta, 1901) up to the most recent releases, developed *ad hoc* for seismic hazard purposes. (Camassi and Stucchi, 1997; Working Group CPTI, 1999, 2004). Also some instrumental databases are available, which cover the whole country or particular seismic sequences (e.g., Working Group CSTI, 2001; Selvaggi *et al.*, 2002; Castello *et al.*, 2005). A short presentation follows.

The CPTI Earthquake Catalog

The first version of CPTI catalog (Working Group CPTI, 1999) is a compilation obtained by merging the data sets (namely NT4.1 stays for Camassi and Stucchi, 1997; Catalogo dei Forti Terremoti Italiani (CFTI) for Boschi *et al.*, 1995; 1997) collected independently by national institutions during the 1990s; in its principal section it describes 2480 earthquakes from the second century B.C. to 1992. In 2004, a new version has been released: it reports earthquakes until 2002 (Working Group CPTI, 2004). The compilations maintain the hazard-oriented choices done by the NT4.1 historical catalog, retaining only independent earthquakes over the damage threshold ($I_o \geq$ V/VI MCS, or $M \geq 4.0$); the foreshock and aftershock removal is done with a "simple" 90-day and 30-km distance window. The first version reports out-of-criteria events in separate appendices. Most of the events being historical ones, the parameters are homogeneously derived from macroseismic data; location and epicentral intensity is mainly derived from the distribution of the highest intensity points. In the 1999 version four types of magnitude are given, computed from macroseismic equivalence (M_e, M_m), obtained by instrumental data (M_s) or as "weighted mean" (M_a): the dispersion of these estimates is, in general, very limited and is always in the range of experimental uncertainties. The 2004 version keeps only M_a and introduces some columns of derived magnitude for hazard computation (see the catalogs for further details). The central Apennines are probably the region where seismological data collection is more reliable and complete. This consideration does not exclude that events may be missing or mislocated and that completeness is not homogeneous for all magnitudes. Data completeness is quite a complex issue, which has serious consequences in terms of balance of seismic moment release. This aspect, explored in previous analyses (Peruzza, 1999; Peruzza and Pace, 2002), is outside the scope of this article and will only be mentioned here.

Several tests have been done for the study area (latitude from 41.5° to 44.5° N, longitude 11.5° to 14.5° E) by (1) plotting the cumulative number of earthquakes versus time (N_{cum} plots), above given magnitude thresholds; (2) plotting the seismic moment release in time and space (computed on grid points using variable search distance and time and referring the seismic moment release to unit time and unit area). The discontinuities in the slope of N_{cum} plots indicate the data set complete from 1000 to 1200 A.D. onward for the highest magnitude ($M_a \geq 6.4$ corresponding to IX–X MCS), and from 1500 to 1600 onward for $M_a > 5.5$ (VIII MCS). Below this value, completeness is limited to much shorter periods. In addition, the seismic moment release has been quite homogeneous since the seventeenth century, but a similar slope is also present around the fourteenth century.

Historical considerations prompt us, therefore, to approximate data completeness to 1000 years, for $M_a \geq 6.4$ and to 400 years for $M_a \geq 5.6$, the same criteria adopted in previous studies using the NT4.1 catalog (Peruzza, 1999; Pace *et al.*, 2002b): we stress that in this area most of the records of the CPTI catalog derive from the NT4.1, but the energetic content expressed by the M_a value is slightly higher than those of M_m reported in NT4.1. The CPTI catalog has been used to associate events to the seismogenic boxes (see Fig. 3 and Table 2) and to parameterize the seismicity models of the seismotectonic provinces.

The Instrumental Earthquake Databases

Two compilations of instrumental records on a national scale have been analyzed in this study, plus some studies on the Umbria-Marche 1997–1998 seismic sequence.

The first one is the instrumental catalog released in 2001 by Working Group CSTI; it collects and uniformly describes the data recorded by the national and local networks from 1981 to 1996. The catalog has about 34,700 events with an associated magnitude (mainly computed from duration); earthquakes with $M < 2.0$ are strongly affected by incompleteness, but the data set may be incomplete locally even for magnitudes as high as 2.5–2.8, as the quality of instrumental coverage has been constantly improving. The time span of the catalog covers some seismic crises that occurred in the region like that affecting the Gubbio area in April 1984 and the Val di Sangro area in May 1984, but with a resolution power of the network that has strongly varied in time.

The most recent instrumental earthquake catalog is the one compiled in the frame of a 4-year project funded by the National Civil Protection Department (Amato and Selvaggi, 2004) and it was published very recently (Castello *et al.*, 2005). The Catalogo della Sismicità Italiana (CSI) catalog refers to a longer period (1981–2002) and therefore covers the 1997–1998 Umbria-Marche seismic sequence. The global number of located events is two times greater than CSTI catalog (99,780 compared with 46,701), but in the study area only about 60% of the locations have an associated magnitude estimate during the period covered by both the catalogs (11,706 events in CSTI; 6839 in CSI); the increased level of the seismic activity since 1997 and the temporary networks installed in the Colfiorito area account for the other 10,815 events with a magnitude estimate listed in CSI from 1997 until 2002. Magnitude distributions in the study area in both the catalogs exhibit a peak on M 1.7–1.8. We will see afterward how these additional 6 years of seismic monitoring influence the characterization of the low-level seismicity.

These databases contain foreshocks and aftershocks, and therefore they are not suitable for use in traditional seismic-hazard analyses that consider independent events only. We therefore processed the catalog for fore- and aftershock removal. We discarded the "cold" criteria used by the historical catalogs, and we abandoned also some well-known filtering algorithms used in the literature (Gardner and Knopoff, 1974; Knopoff *et al.*, 1982; Slejko and Rebez, 2002, developed for northeastern Italy), because they turned out to be too rigid if applied to low-magnitude data sets. We used, therefore, the original table proposed by Knopoff (2000), extended downward to magnitude M 3 by interpolating it in the form of the following relationships:

$$\mathrm{Log}(T) = 0.725M - 2.007 \tag{1}$$

$$\mathrm{Log}(D) = 0.347M - 0.567 \tag{2}$$

where the time T is expressed in days, and the distance D is in kilometers. Finally, we tested the Reasenberg filtering procedure (Reasenberg, 1985; Reasenberg and Jones, 1989, 1994; see also Lolli and Gasperini, 2003, for the application in Italy), using the Fortran code *Cluster2000* freely available at the U.S. Geological Survey site (http://quake.wr.usgs.gov/research/software/, last accessed July 2005).

We found that the best filtering algorithm is the empirically based step function used by Knopoff (2000), because it is capable of preserving the main features of the instrumental seismicity in the central Apennines, often done by long-lasting swarms. In fact, these simple formulas, applied to both the instrumental catalogs, obtain a filtered data set of earthquakes very similar to that obtained by using the Reasenberg procedure (24,850 CSI events with $M > 2.0$ became 18,852 or 18,789 using the Reasenberg or Knopoff methods, respectively; with CSTI, the $M > 2.0$ original 17,365 events remain 15,475 and 15,364; Fig. 2), with significant consequences for the estimates of the seismicity levels in the area. When the filtering algorithms are used on a single seismic sequence (we tested the Umbria-Marche sequence of 1997–1998; data from Selvaggi *et al.*, 2002), the aftershock removal proposed by equations (1) and (2) recognizes all the major shocks corresponding to distinct ruptures of fault segments as "main events," more effectively than the Reasenberg procedure, guaranteeing that the complex faulting pattern is represented by "independent" events.

Seismic-Source Modeling

Seismic-source modeling drives the results of seismic-hazard analyses. In this section, we quantify the expected seismicity of the study area in terms of geometry and rates of the sources, separating them into three layers that use different methods to constrain the seismicity rates in relation to the available data. The description moves from the better-known seismogenic sources to the less defined ones.

Seismogenic Boxes: Medium-to-Large Earthquakes Linked to Individual Structures

Source characterization of a fault consists in quantifying the magnitude distribution of the segment and in defining their occurrence model. In this section we will try to infer the long-term seismic potential of fault segments using the seismogenic boxes defined in Figure 3 and the geometric parameters and observations gathered in Tables 1 and 2.

Various types of primary observations have been used in literature to estimate the magnitudes of earthquakes not detected by instruments and, therefore, to infer the maximum expected magnitude (M_{max}) on a fault segment; the mean coseismic displacement on the fault trace and the size of the surface or subsurface fault are by far the most commonly used parameters. In Italy, and in particular, in the central Apennines, observations of coseismic displacement are rare; the full 3D geometry of the seismogenic fault is therefore the best way to get a M_{max} estimate.

Using the approach tested in previous articles (Pace *et al.*, 2002b; Peruzza and Pace, 2002), we calculated for each seismogenic box the M_{max} values with empirical relationships calibrated on normal faulting (Wells and Coppersmith,

1994) by using the maximum subsurface fault length and area (respectively, L and RA in Table 1). We derived M_{max} also from the relationships between fault dimensions and scalar seismic moment (M_0) expressed by:

$$M_0 = GDLW = GkL^2W, \quad (3)$$

where L, W, and D are, respectively the along-strike rupture length, down-dip width, and average displacement of a rectangular source. G is the rigidity modulus ($3 \cdot 10^{10}$ Pa for crustal rocks; Hanks and Kanamori, 1979), and k is the strain drop, defined as the displacement to length ratio (D/L). Accepting the reasonable assumption that strain drop is constant in homogeneous seismotectonic regions (Scholz, 1990) and using the value $k = 3 \cdot 10^{-5}$ obtained by Selvaggi (1998) for normal faulting earthquakes in the Apennines, we can derive M_0 estimates without having reliable D values.

After having calibrated a regression relationship of L versus W on about 180 earthquakes around the world (see Peruzza and Pace, 2002, for details), we corrected the maximum possible along-strike rupture as a function of down-dip extension of the fault ("corrected length") and so the M_{max} values of the more shallow sources (e.g., the Valle Umbra sources, SBs 16 and 17); we obtain more reasonable M_{max} values, which are comparable to the observed historical and instrumental earthquakes.

Figure 4 shows the M_{max} values computed for each seismogenic box and compares them with the associated earthquakes (see also Table 2). For SBs 4, 8, 16, 17, 19, 26, and 27 we used the corrected lengths reported in parentheses in Table 1. The dispersion of the computed M_{max} values is fairly small (a maximum scatter of about 0.3) and is fully comparable with instrumental uncertainties. In 11 of 28 seismogenic boxes a maximum event of M_{max} occurred during historical times, following our proposed earthquake-box association. Only in the case of the 1915 earthquake, in SB 22, did the observed magnitude significantly exceed the calculated one. The instrumental magnitude (Margottini *et al.*, 1993, referenced in the previous catalog NT4.1, Camassi and Stucchi, 1997) is derived from 22 recordings with an associated standard deviation of 0.74, and it is classified as a M_s type: accepting the equivalence in the definition of M_s and M_w in the range 6–7.5 (e.g., Ekström and Dziewonski, 1988), the difference (M_{max} observed of 7.0 against 6.6 computed) is inside the aleatoric uncertainty. Using geodetic observations, Ward and Valensise (1989) estimated a M_w close to 6.6, similar to that obtained by Amoruso *et al.* (1998) using a nonlinear inversion approach that takes into account both near-field surface deformations and far-field first-motion polarities; they identified a fault length parameter of ≈24 km, a value close to the coseismic rupture recognized by Oddone (1915) and to the length assigned to SB 22 in this study (Table 1).

Then, to enhance the use of the geometric and kinematic parameters assigned to the boxes and to have an independent constraint to the seismic characterization, we calculated the mean recurrence time ($T_{M_{max}}$) of the maximum event in each source; we did it indirectly, because for most of the SBs we do not have recurrence intervals or paleoseismological observations providing reliable mean values.

We estimate the $T_{M_{max}}$ using two different techniques. The first one obtains the values of $T_{M_{max}}$ using the criterion of the "segment seismic moment conservation," proposed by Field *et al.* (1999):

$$1/T_{M_{max}} = \text{Char\_Rate} = G \cdot \text{SE} \cdot L \cdot \text{SR}/10^{(1.5M+9.05)} \quad (4)$$

where Char_Rate is the annual rate of earthquakes on that source, G is the rigidity modulus, SE is the slip per event, L is the length, and SR is the averaged (or long-term) slip rate. The second technique is the simple ratio $T = \text{SE/SR}$. Slip rates derive from neotectonic and paleoseismological studies (references in Table 1), whereas the slip-per-event values derive homogeneously from empirical relationships (Wells and Coppersmith, 1994) after a comparison with the few available paleoseismological data (Pantosti *et al.*, 1996; Michetti *et al.*, 1996; D'Addezio *et al.*, 2001).

Figure 5 shows the $T_{M_{max}}$ calculated for each seismogenic box, using the two different methods and the three M_{max} values of Figure 4. The recurrence time estimates vary significantly, about 30% of the mean values (about 300 years over 1000, with some of the worst cases in SBs 2, 26, and 27).

Without using equation (4), the values are less scattered (about 10–15%), but the slip's ratio method is only apparently more accurate, because all the slip-per-event values are inferred. The variations derive only from the magnitude dispersion entered in the scaling laws used for computing the slip-per-event values, because the slip rate is fixed; the actual uncertainties are therefore much higher, and the values obtained here have to be considered only as a first step toward solving the problem. The statistics on $T_{M_{max}}$ values are given in Table 3; the mean of the maximum event's recurrence times is plotted in Figure 5 with a filled, inverted triangle: it will be used later on to characterize the distribution functions for the time-dependent seismic-hazard assessment.

Magnitudes from seismic moment (M 3 in Fig. 4) and their related recurrence times, calculated using the "segment seismic moment conservation" criterion (T6 in Fig. 5), will be used in the following text to parameterize the whole seismic activity of the seismogenic boxes. By far, M_{max} and $T_{M_{max}}$ are the least constrained parameters available, but the geological observations, coupled with the seismological data, are the only way to constrain the model of long recurrences of the maximum events, as is necessary in seismic-hazard assessment.

With regard to the occurrence model, the literature includes two very diverse approaches in dealing with the mechanical behavior of faults. Some models assume that individual faults, or fault segments, essentially tend to generate the same-size earthquakes or characteristic ones with a relatively narrow range of magnitude at or near the M_{max} (e.g.,

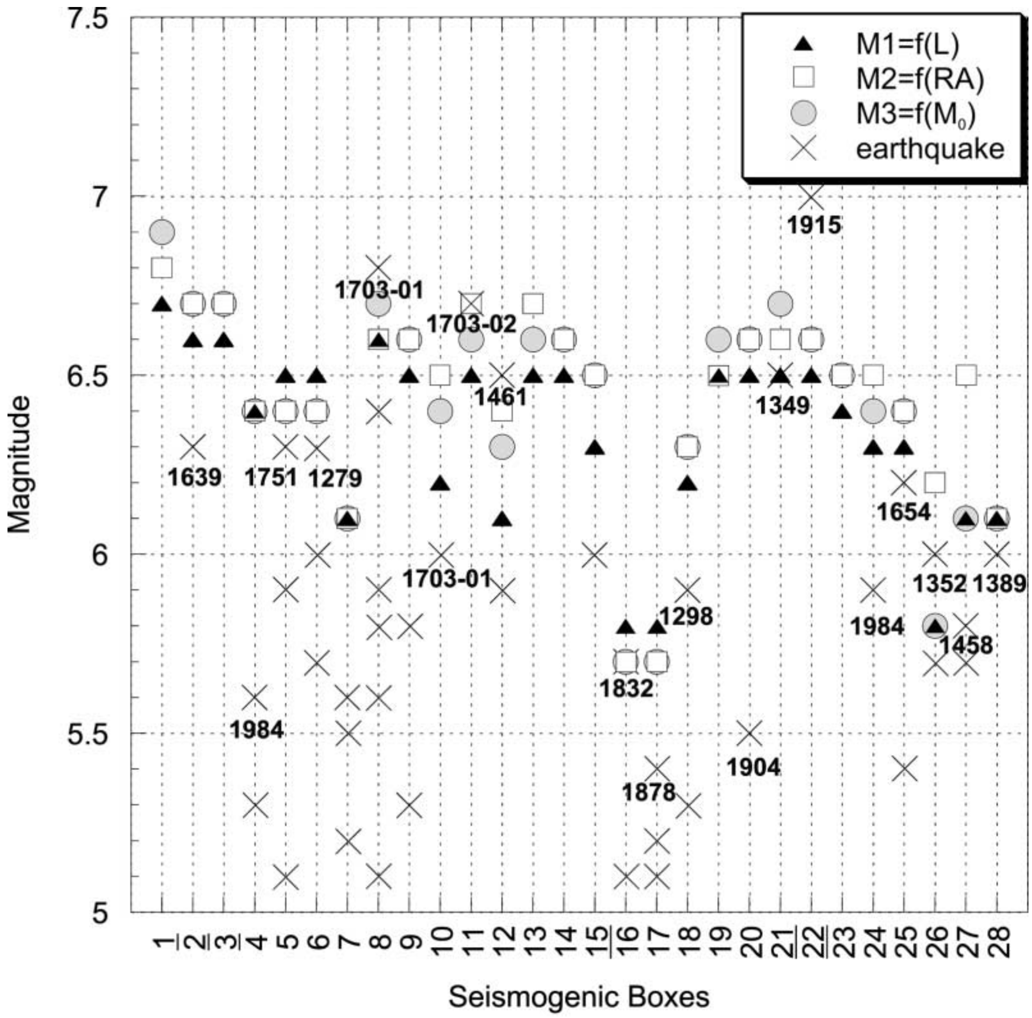

Figure 4. Maximum expected magnitude ($M_{\max}$) calculated for the seismogenic boxes in central Italy. Legend is as follows: M1 is M_w from master fault length (L, see Table 1) by using the Wells and Coppersmith (1994) empirical relations on subsurface rupture length (RLD); M2 is M_w as before, using the master fault rupture area (RA); M3 is M_w from the scalar seismic moment of equation (3), assuming a constant strain drop. The most important historical and instrumental earthquakes associated with the SBs (see Table 2) are marked by crosses; the source code is underlined for boxes with paleoseismologically observed earthquakes (Table 2).

the characteristic earthquake model of Schwartz and Coppersmith, 1984). These models are essentially driven by geological observations where, at a point along a fault, the displacement during successive surface-faulting earthquakes remained more or less constant. Some other models, essentially derived by statistical studies of the seismicity distribution in a region, assume that the number of earthquakes from a single source/fault is exponentially distributed with earthquake magnitude. The general form of these recurrence models is the well-known Gutenberg-Richter (G-R) relation (Gutenberg and Richter, 1944):

$$\operatorname{Log} N = a - bM, \tag{5}$$

where N is the number of events with a magnitude greater than or equal to M, and a and b are empirical constants.

A priori, for each seismogenic box we decided to use one of these two well-known earthquake recurrence models. For the sources that have a nearly continuous spectrum of magnitudes documented by seismological observations, we adopted the G-R model. The G-R distribution is anchored and truncated on the different ($M_{\max}$, $1/T_{M_{\max}}$) values of the boxes and has a constant $b = 1.0$; this value was obtained by the G-R interpolation of all the earthquakes occurring in the Apennine extensional seismotectonic province (SP B, described in Fig. 7), as single boxes are insufficient for statistics. For the SBs in which single-value magnitudes prevail, we use the "characteristic earthquake" model (CH): the oc-

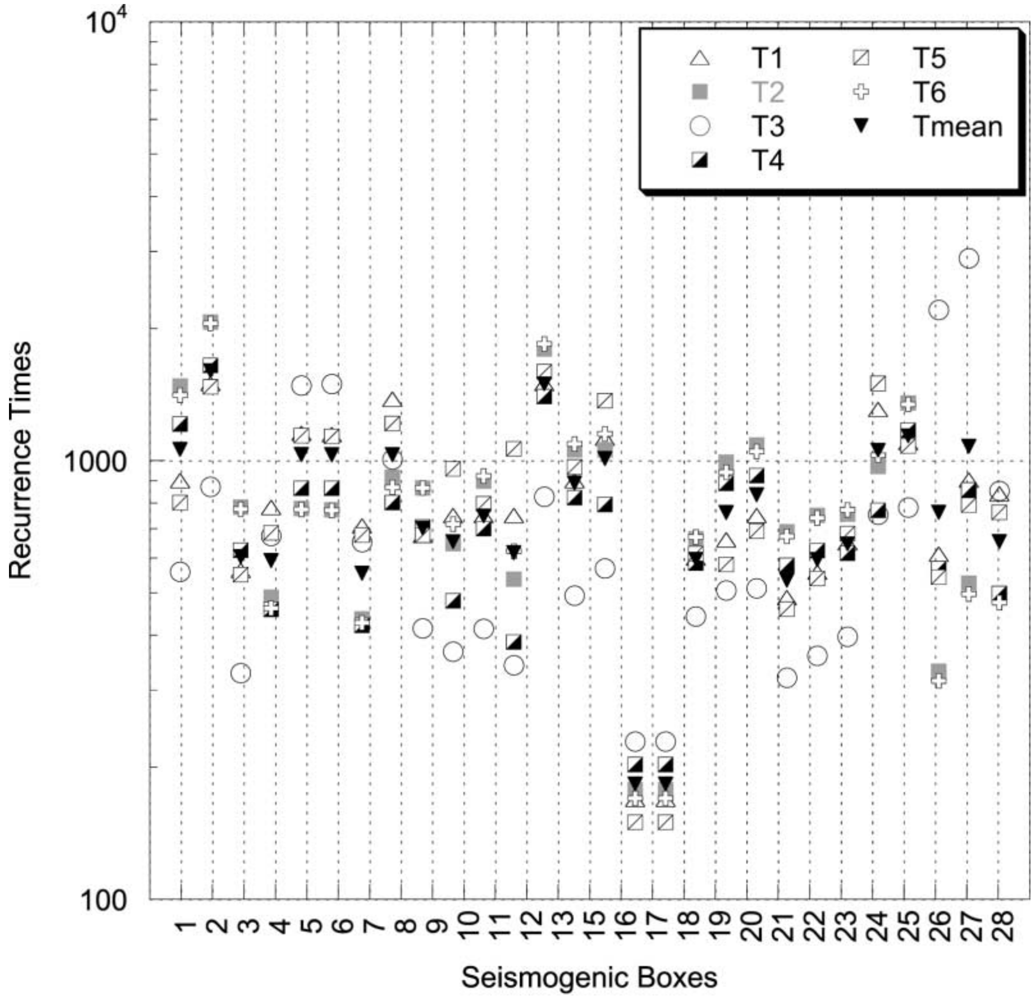

Figure 5. Mean recurrence times ($T_{M_{max}}$) associated with the maximum expected earthquake for SBs in central Italy; values T1–T3 are obtained by $T = SE/SR$ (slip-ratio method) using, respectively, M1, M2, and M3 and the related SE from the Wells and Coppersmith (1994) relationships. Values T4–T6 use equation (4) (seismic-moment conservation method) as before; T_{mean} are the mean values (see Table 3).

currences are calculated by a truncated Gaussian distribution, peaked on M_{max} and $T_{M_{max}}$, with a σ value of 0.3, representing a simplified estimate of M_{max} uncertainties. A small tail of G-R exponential distribution models the queue of low magnitude for these sources; it is anchored to the rate of occurrence of moderate events and has a constant $b = 1.0$, if magnitudes as low as 0.5–0.7 compared to M_{max} have been observed, but with an occurrence rate much lower than that predicted with the simpler G-R model: we name this behavior "Hybrid" according to the definition given by Wu *et al.* (1995). If no earthquakes with $M > 4.5$ have been reported by historical and instrumental catalogs, the tail is modeled only in terms of cells of variable *a* and *b* values, as depicted by the contribution of the background instrumental seismicity described later on; we classify these sources as pure characteristic earthquake sources. The type of model used for the seismogenic boxes is indicated in Table 3.

Having chosen the occurrence model, and given a calibration point (M_{max}, $1/T_{M_{max}}$) to the model, we can derive straightforwardly the seismicity rates of the seismogenic boxes by imposing a seismic-moment budget. The assumption of seismic-moment conservation is easy to comprehend if we consider the pure characteristic earthquake model, where a spike of seismicity corresponds to the characteristic event. If, instead of using a spike, we model the characteristic earthquake rates with a peaked Gaussian distribution function, we have to impose the condition that the total amount of seismic moment released by the fault system (e.g., some magnitude classes around the M_{char} value) does not exceed the seismic moment released by the characteristic magnitude alone, whatever the magnitude-sampling factor of the Gaussian function is (here the step chosen is 0.3). Similarly, when we use a G-R distribution, the sampling factor controls the total amount of energy released. Therefore, it is necessary to impose the condition that the total amount of seismic moment released in a given period by the distri-

Table 3
Hazard Input Parameters for the Seismogenic Boxes*

	Seismogenic Boxes	M_{max} M3	$T_{M_{max}}$ T6	Statistics on $T_{M_{max}}$ Minimum	Maximum	Mean	Median	Variance	Std Error	α	Model	T_{dep}
1	Bove-Vettore	6.9	900	558	1480	1060.2	1055.5	1.33E+05	148.98	0.34	CH	yes
2	Gorzano	6.7	1500	872	2070	1603.2	1574.0	1.97E+05	181.29	0.28	HY	yes
3	Gran Sasso	6.7	562	328	784	604.2	593.5	28,656	69.109	0.28	CH	yes
4	Gubbio	6.4	782	458	782	591.3	581.0	19,481	56.981	0.24	GR	no
5	Gualdo Tadino	6.4	1155	774	1484	1032.8	1003.0	78,056	114.06	0.27	HY	yes
6	Colfiorito	6.4	1146	770	1496	1031.0	1000.5	80,543	115.86	0.28	CH	yes
7	S. Martino-Civitella	6.1	710	421	710	553.8	544.0	19,362	56.807	0.25	GR	no
8	Nottoria-Preci	6.7	1381	802	1381	1031.7	961.5	49,732	91.042	0.22	HY	yes
9	Cascia-Cittareale	6.6	675	415	866	700.7	691.0	27,514	67.718	0.24	HY	yes
10	Montereale	6.4	750	367	958	653.0	682.0	43,728	85.369	0.32	CH	yes
11	Pizzoli-Pettino	6.6	750	414	922	747.2	774.0	33,887	75.152	0.25	CH	yes
12	Paganica	6.3	750	342	1064	616.8	579.5	70,582	108.46	0.43	CH	yes
13	Media Valle Aterno	6.6	1500	828	1844	1494.0	1547.5	1.35E+05	150.22	0.25	CH	no
14	Sulmona	6.6	900	493	1092	889.0	933.5	47,497	88.973	0.25	CH	yes
15	Pizzalto-Cinquemiglia	6.5	1125	568	1370	1011.0	1092.0	81,368	116.45	0.28	CH	yes
16	Valle Umbra N	5.7	169	150	229	183.2	174.0	798.97	11.54	0.15	GR	no
17	Valle Umbra S	5.7	169	150	229	183.2	174.0	798.97	11.54	0.15	GR	no
18	Rieti	6.3	600	442	670	595.7	607.0	6,859.9	33.813	0.14	HY	no
19	Valle del Salto	6.6	660	506	993	761.3	774.0	42,068	83.734	0.27	CH	no
20	Velino-Magnola	6.6	750	512	1086	835.5	837.5	49,837	91.138	0.27	HY	no
21	Campo Felice-Ovindoli	6.7	487	320	689	534.0	532.0	19,710	57.314	0.26	CH	yes
22	Fucino	6.6	557	359	751	595.0	590.5	21,296	59.576	0.25	CH	yes
23	M. Marsicano	6.5	650	397	772	645.3	666.0	18,449	55.452	0.21	CH	no
24	Barrea	6.4	1308	753	1500	1055.2	1000.0	88,439	121.41	0.28	GR	no
25	Sora	6.4	1100	782	1354	1139.0	1136.5	44,348	85.973	0.18	HY	no
26	M.S. Maria Tiberina	5.8	612	315	2206	762.3	555.0	5.16E+05	293.21	0.94	CH	yes
27	Città di Castello	6.1	903	497	2892	1077.8	824.5	8.19E+05	369.42	0.84	HY	yes
28	Parnacciano	6.1	840	475	853	653.8	630.0	33,504	74.726	0.28	HY	yes

*The selected maximum expected magnitude (M_{max}) and associated recurrence time ($T_{M_{max}}$) are, respectively, *M*3 in Figure 4 and T6 in Figure 5. The statistics on the different recurrence times associated with the maximum expected earthquake lets us obtain the aperiodicity value α, used by the time-dependent (T_{dep}) approach (yes or no in the last column). The type of model chosen for the seismogenic boxes is as follows: GR, Gutenberg-Richter exponential distribution function; CH, bell-shaped approximation of a characteristic earthquake model; HY, hybrid model with a characteristic peak and a GR tail for smaller magnitude.

bution (sampled magnitude) is equal to the moment released by the maximum expected earthquake, at the same time. The seismic-moment conservation is therefore done by (1) fixing the budget of seismic-moment release in terms of the seismic-moment rate given by the maximum expected earthquake (i.e., $M_0[M_{max}]$ in $T_{M_{max}}$ years) and (2) scaling the occurrences of each magnitude class in such a way that the summation of seismic-moment rates over all the classes equals the seismic-moment rate obtained from the maximum expected earthquake. In the future, geodetic data (e.g., Hunstad *et al.*, 2003) will provide additional constraints in performing seismic-moment budgeting, which has never been applied in Italy until now.

Figure 6 reports some examples of seismicity rates, computed by using different occurrence models and compared with instrumental rates (earthquakes located inside each seismogenic box by Working Group CSTI [2001] and by Castello *et al.* [2005]). Working on such a detailed scale, we recognize that epicentral locations may sometimes be affected by uncertainties because of the spacing of stations of the national seismic network. This is the case, for example, of the mainshock (M_s 5.8) of the 1984 Val di Sangro sequence, whose location is quite uncertain and lies outside the SB 24 polygon; the temporary stations installed in the area after the main event depicted the true geometry of the source (Pace *et al.*, 2002a). The two instrumental catalogs (CSTI and CSI; Fig. 6) give similar rates for the sources not involved in the 1997–1998 seismic sequences; in the epicentral region (SB 6) the G-R slope is quite impressively constant ($b \approx 0.9$), with an evident bulk at $M > 5$. We attribute these differences to the changes in the geometry of the network and in the processing of the data.

The graphs suggest that careful selection of the recurrence models, constrained by the geometry and kinematics of the individual sources, may give reasonable seismicity rates; they can be extrapolated for low magnitudes too, giving rates that agree with those derived from short instrumental monitoring. The time-dependent seismicity rates (plusses in Fig. 6, reported for some sources) will be described later.

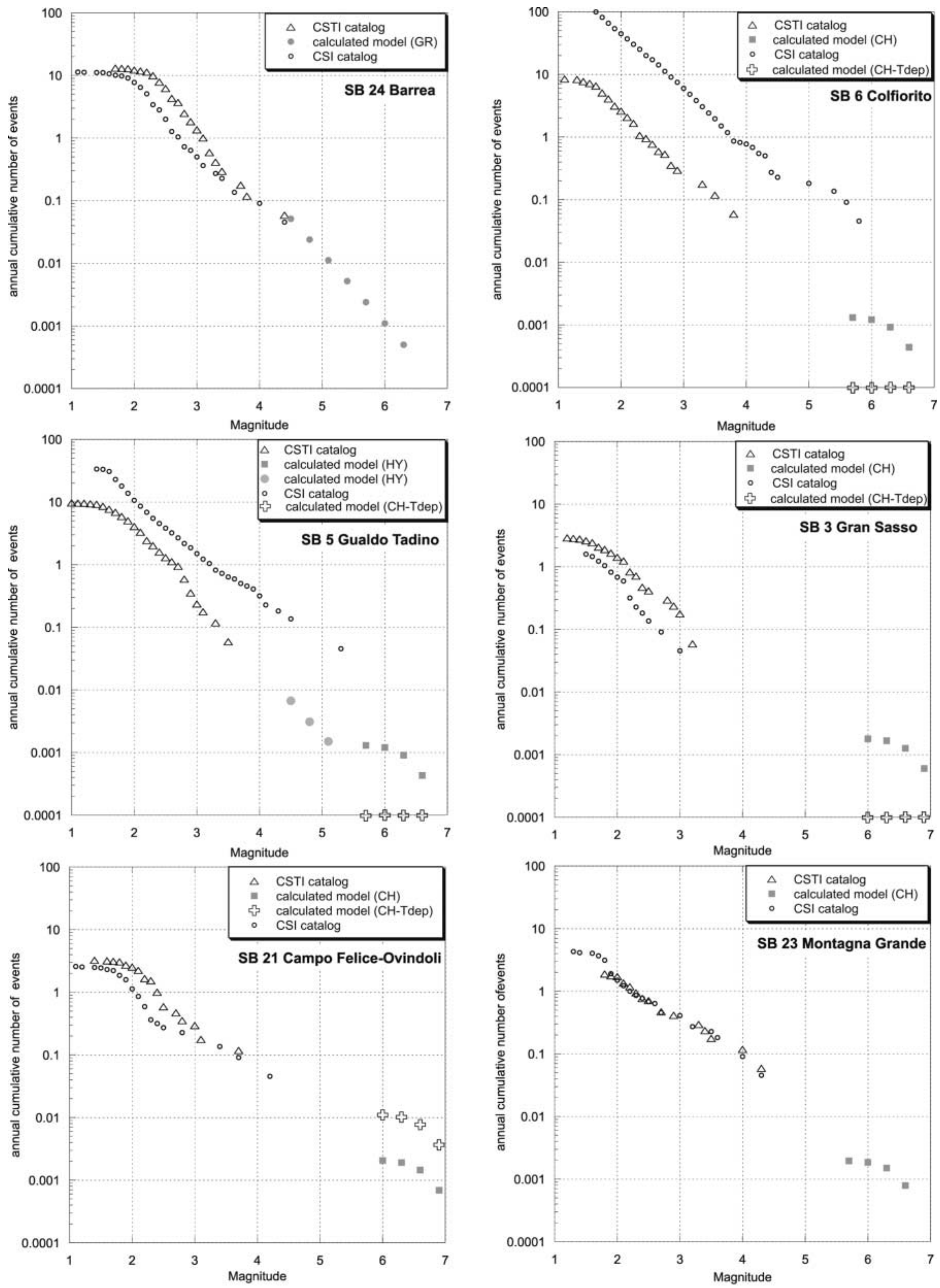

Figure 6. Examples of seismicity rates of some seismogenic boxes in central Italy. Observed rates (triangles and circles) represent the annual cumulative number of events located inside the box, according to the instrumental database CSTI (Working Group CSTI, 2001) and CSI (Castello *et al.*, 2005). The computed rates (gray dots and squares) derive from the *a priori* selected model, combined with the geological constraints (see the text); plusses represent time-dependent rates (null if plotted on the *x* axis).

Seismotectonic Provinces: Diffuse Seismicity on Large Areas

The seismotectonic provinces previously described were used to model the earthquake occurrences with $M \geq 5.5$ that are not directly correlated to individual seismogenic sources. In fact, no seismogenic boxes in SPs A, C, and D are supported by independent geological and/or paleoseismological information.

As common practice in the requirements of PSH studies, we extracted the earthquakes located inside the polygons, representing seismotectonic provinces, to get statistics from them. All the seismological databases were used, the two instrumental catalogs (namely CSTI and CSI), declustered for aftershock removal, and the historical CPTI catalog, in adequate time windows. As previously stated, data completeness for the CPTI database is taken from the past 400 years for $M < 6.4$ and 1000 years for $M \geq 6.4$; below M 5.5 this data set can be not complete. The instrumental catalogs are considered complete for the periods they refer to (16 years for CSTI, 22 years for CSI); magnitudes lower than 2.0 and events deeper than 50 km have been discarded from our completeness analysis. The historical and instrumental databases overlap in time namely for $M > 4.0$.

The G-R relationships for each province have been obtained by interpolating the cumulative annual number of events with the least-squares (lsq) and the maximum likelihood (mlk) methods (Aki, 1965; Utsu, 1965, 1966; Weichert, 1980), obtaining the a (normalized to 1 year) and b coefficients. The distributions obtained from historical and instrumental databases (Fig. 7) are properly connected; it suggests that the periods selected for data completeness are adequate, and no discontinuities in the magnitude estimate between the historical and instrumental records are evident.

The seismic crisis that occurred in the Umbria-Marche region in 1997–1998 is not represented by the CSTI data, but the CSTI and CSI instrumental data sets are rather impressively similar in SP B and C, in the provinces where the crisis occurred, whereas in SP A and D, the rate of activity (a value in the G-R relation) is lower in the longest catalog (CSI) for normalization reasons. This analysis confirms the invariance of the G-R with respect to the Umbria-Marche sequence, the strongest that occurred in Italy after the 1980 (M_s 6.9) Irpinia earthquake, as already demonstrated by previous analyses of the data recorded by local and temporary networks (see Peruzza, 1999; Cattaneo *et al.*, 2000). These considerations lead us to prefer the CSTI catalog, as less influenced by heterogeneity in the monitoring network; the G-R relationships obtained by CSTI (lsq coefficients reported in Fig. 7) can be considered representative of the seismicity of the province for magnitude below approximately 5.0–5.5. At higher magnitude, the seismicity rates of the provinces are better represented by the historical catalog CPTI. The G-R relationships obtained by the least-squares method on $M > 4.5$ are reported in Figure 7 also.

Three provinces (C, D, and, in part, B) present a bulk departure from a G-R trend; it may be both the expression of "characteristic earthquake" behavior of individual sources inside the province, or the consequence of "clustering" in magnitude classes due to the use of macroseismic data. The identification of individual seismogenic boxes in SP C and D will probably help to solve this question in the future.

For the Apennine extensional SP B, in Figure 7, we also reported the sum of the rates calculated from the "geological" seismic-source modeling of the seismogenic boxes. This graph demonstrates that individual sources alone are capable of explaining all the observed seismicity and in some magnitude classes even to overcome it; historical rates (clustered with the same step used for the seismogenic boxes, white plusses in Fig. 7b) are lower than the "geological" rates for $M \sim> 5.5$ and at M 4.5 also. This scenario is compatible with the lack of experimental data because of incompleteness (missing earthquakes in the past 400 years for low M and seismic sources not active in the last 1000 years for the highest M). We stress again that the seismicity rates of the seismogenic boxes and those of the provinces follow different assumptions. In the first case, we keep the seismic-moment rate of each individual source constant; while using earthquake statistics on wide-area sources, we conserve the seismicity rates. The good agreement between experimental (historical rates) and modeled data (Σ of the geological rates) in Figure 7b makes us consider the seismotectonic constraints adopted to quantify the seismicity in this sector of the Apennine chain reliable. As already stated, additional studies are necessary to increase our knowledge of the other provinces. To evaluate the probabilistic seismic hazard of the seismotectonic provinces A, C, and D, we can now only use the experimental data; the expected seismicity rates have been calculated for $M \geq 5.5$ by the G-R relationships derived from the CPTI catalog. For reasons of caution, we truncated the distribution to a maximum magnitude value corresponding to a mean recurrence time of ~1000 years.

Grid Elementary Sources for Low-Level Background Seismicity

The third layer of seismic sources is related to medium-to-low seismicity, an energetic level that usually receives less attention in Italian PSH analyses, but it has a strong relevance for high-vulnerability areas, such as most of the historical towns in central Italy. The medium-to-low seismicity ($2 \leq M < 5.5$, herein referred as "background" seismicity) is modeled on the instrumental catalogs available, following a philosophy similar to that adopted by "spatially smoothed seismicity" techniques (e.g., Frankel, 1995). In fact, the basic assumption of homogeneously distributed seismicity is a necessary but simplistic approximation, bypassed by the increase of knowledge; small-magnitude events do not usually leave a geological record, and macroseismic data may be dominated by effects not related to the source; therefore, only the instrumental seismological data

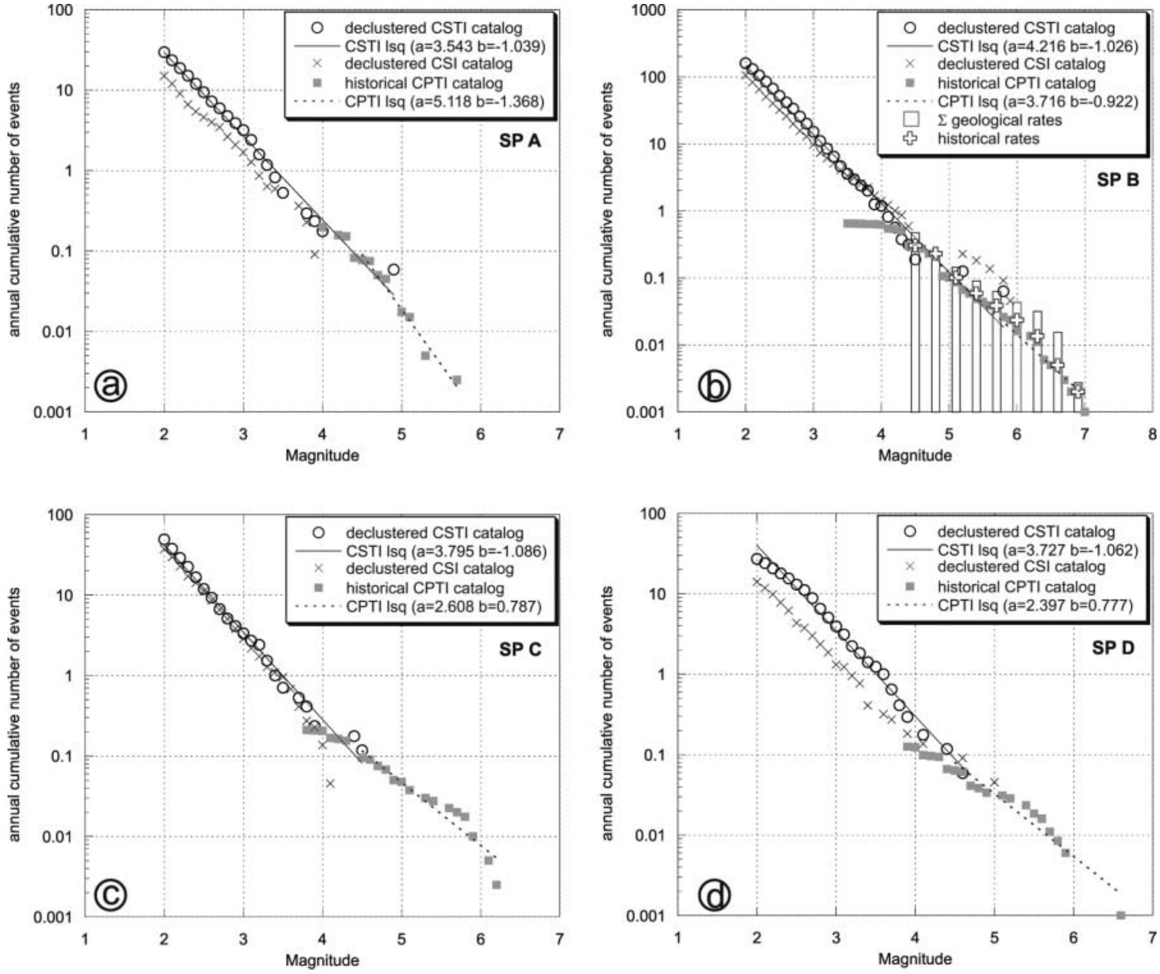

Figure 7. Seismicity rates associated to the four seismotectonic provinces in central Italy. Instrumental and historical catalogs (CSTI for Working Group CSTI, 2001; CSI for Castello *et al.*, 2005; CPTI for Working Group CPTI, 2004) have been used; G-R relationship is interpolated by using the least-squares (lsq) method. Bars in SP B represent the summation of the rates of the 28 seismogenic boxes computed using the geological information; plusses are the CPTI rates aggregated with the same magnitude step (0.3).

can be representative of the spatial distribution of minor seismicity to describe local variations (e.g., the limits of volcanic districts, inside SP A). Using the declustered instrumental catalogs, we extracted groups of seismic events within a given distance from a grid point to compute *a* and *b* coefficients of the G-R relationship. After a sensitivity analysis, we chose a grid node spacing of 0.1° both in longitude and in latitude (corresponding roughly to 7–11 km) and a search radius of 20 km. This value represents a compromise between the requirements for statistics and the detail of lateral variation of the seismic characters. The partial overlap of the circular search areas smoothes the differences between adjacent nodes of the grid. Data interpolation to obtain the G-R relationship coefficients has been done using the traditional algorithms of least squares (lsq) and maximum likelihood (mlk) (Aki, 1965; Utsu, 1965, 1966; Weichert, 1980). The *a* values have been normalized taking into account the time window of the catalogs and the spatial extension of the search areas to represent the "activity rate" of one year and an arbitrary 10 × 10 km unit area.

Figure 8 summarizes the *a* and *b* values distribution in central Italy obtained by the CSTI catalog using the *lsq* method; nodes with less than five events were discarded. Large lateral fluctuations have been obtained for the G-R coefficients, despite the relative stability exhibited by the previous analysis concerning the provinces. These fluctuations may be ascribed both to the characteristics of the seismic activity and of the instrumental network. Using the CSTI catalog we believe we are less influenced by instrumental reasons, as the catalog does not include the 1997–1998 sequence, with the very closely spaced stations installed after the beginning of the seismic crisis (September 1997). We therefore assume that the threshold of earthquake detection of the national seismometric network (Rete Sismica Nazion-

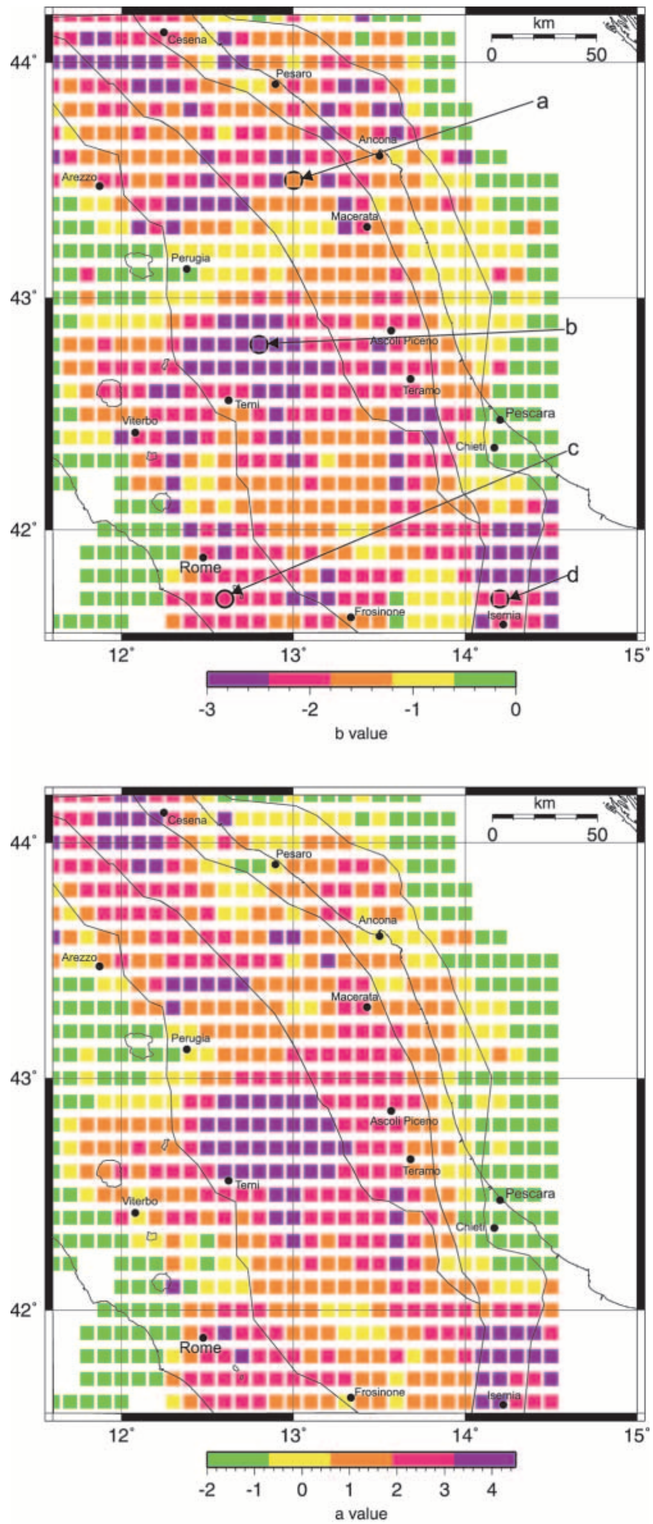

Figure 8. Maps of G-R coefficients in central Italy, using the filtered CSTI catalog. Grid node of 0.1° spacing, search radius of 20 km, least-squares fitting; the *a* values refer to one year and unit area of 100 km^2. The circles indicate the location of data sets shown in Figure 9.

ale Centralizzata [RSNC], www.ingv.it, that integrates some local networks in central Italy) may be considered geometrically and temporally sufficiently homogeneous from 1981 until 1996, with the only exception of some areas close to the coasts. These considerations let us ascribe the lateral variations of the G-R coefficients to the spatial variations of the seismicity. Future efforts to define accurately the spatial and time variations of instrumental completeness will give additional constraints to such analyses.

We note that the regional variations of *a* and *b* values in Figure 8 are in partial agreement with the seismotectonic provinces, defined on a structural-geological data basis; the highest *a* values are mainly concentrated inside the areas of Apennine extensional SP B and the second highest are in the foothill-mixed kinematics SP C. The *a* values, representing the level of seismic activity, follow more or less the same spatial distribution as the *b* values, with higher values (>1) in the axial part of central Italy, close to the Maiella region and in the Colli Albani region (southern area of SP A), and lower values (<1) along the two coasts.

Some examples of G-R fitting are shown in Figure 9 prompting also the choice of the fitting algorithm; they are taken from the northern part of SP C (point a in Fig. 8), the central part of SP B (b), the southern part of SP A (Colli Albani region, c), and in the Maiella region (d). We can clearly see in the graphs that the least-squares (lsq) algorithm fits the experimental data better than the maximum likelihood (mlk) algorithm in the magnitude range $2 < M < 4$. Because it is reasonable to consider this magnitude interval complete, we will use it in our modeling; lower magnitudes can be considered incomplete for instrumental shortcomings, whereas higher magnitudes are incomplete because the temporal window of the catalog (16 years) does not permit us to see the complete seismic process.

The *a* and *b* values of Figure 8 were finally used to compute the seismicity rates of regular adjacent square (in degrees) cells, centered on the mapped nodes. The G-R relationships are extrapolated to the magnitude lower limit that is modeled by the other layers of sources (range 2–5.5 for the provinces A, C, and D; range 2–4.5 for the boxes in SP B). The use of cells of variable *a* and *b* values permits evaluation of the medium-to-low level of expected seismicity, without imposing additional geological evidence, which is difficult to define for some places. Examples are the seismicity correlated to the activity of the Latium active volcanic zones (Colli Albani area) or the seismicity localized in the Maiella region, an area that even today is not very decipherable from a seismotectonic point of view.

PSH Analysis

PSH maps have been designed by using the traditional hypotheses of stationarity and then introducing some simple issues of time dependency. The rates of earthquakes with their pertinent geometries, estimated and described in the preceding section, build the different layers of seismic-

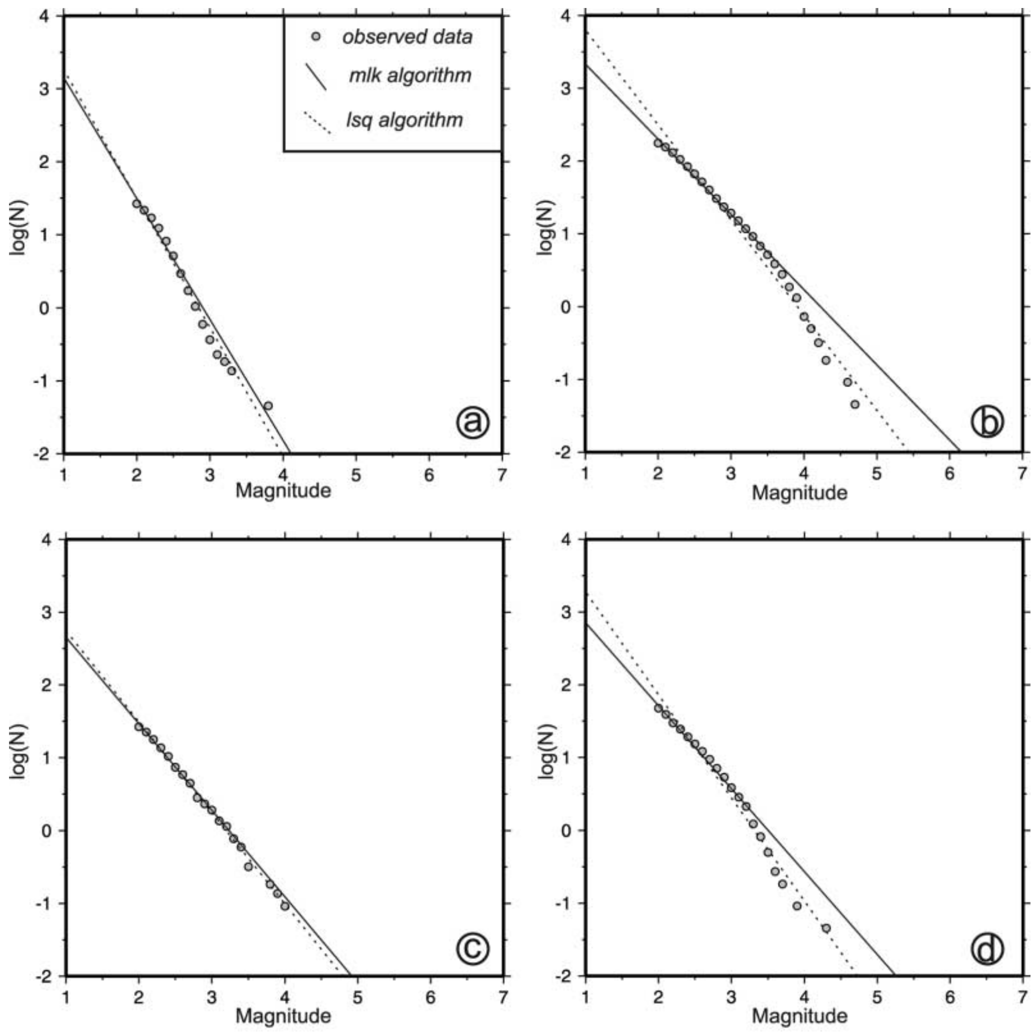

Figure 9. Examples G-R fitting in four nodes in central Italy (location map in Fig. 8). Circles are the earthquakes extracted for the node; full line indicates the relationship obtained using the maximum likelihood (mlk) algorithm and the dashed line indicates the relationship using the least-squares (lsq) method.

hazard assessment. All the computations were performed using the well-known code SEISRISK III (Bender and Perkins, 1987) on a grid spacing 0.05° in latitude and 0.07° in longitude. Results are expressed in peak ground acceleration (PGA) expected not to be exceeded with a probability of 90% in 50 years, in "bedrock" conditions. Attenuation functions are those proposed by Ambraseys *et al.* (1996), based on empirical regressions of the European strong-motion data; the distances used by these authors (distance of the surface projection of fault plane) are compatible with the seismogenic boxes that are surface projections of master faults and get around the problem of handling dipping faults, not solved in SEISRISK III code. The results obtained here are directly comparable with some previous analyses (e.g., Slejko *et al.*, 1998; Lucantoni *et al.*, 2001), yet it is not the same kind of study following the logic tree philosophy or using a semiempirical attenuation function (e.g., Gruppo di Lavoro, 2004). Even if seismic-hazard assessment is very sensitive to attenuation functions, we prefer to focus our attention on the originality of the proposed source model; future implementations will be done according to the needs of the PSH study users. To use low-magnitude seismicity rates we extrapolated the Ambraseys *et al.* relationships downward, so as to avoid the introduction of discontinuities in PGA $= f(D,M)$ modeling (interesting considerations on this subject may be found in Boatwright *et al.*, 2003; Bragato, 2004; and Douglas, 2003). This may cause an overestimation of the hazard for which we partially compensated by the graphical representation, as the PGA results are mapped using quite large, irregular classes (PGA < 0.1, plotted in light blue, they may be roughly considered accelerations that will not cause damages).

The Poisson Hazard Assessment

Poisson hazard assessments are those obtained through the use of the three levels of seismic sources previously described, accepting the assumption of stationarity of seismicity. The results are illustrated in Figures 10 and 11.

In Figure 10a we mapped the contribution to hazard of the layer defined as low-level background seismicity; in Figure 10b the source model refers to the layers of the seismotectonic provinces (SP A, C, and D) and of the seismogenic boxes (inside SP B). Figure 11 reports the global results deriving from all three layers of seismic-source modeling. PGA values include the uncertainties in attenuation.

The background seismicity (Fig. 10a) is modeled using the seismicity rates coming from G-R interpolation of instrumental recent seismicity in the magnitude range 2–5.5; in the Apennine extensional SP B area we considered only the interval $2 \leq M < 4.5$ to use the SBs model rates completely. Despite this choice, and despite the fact that the 1997–1998 seismic crisis in the Umbria-Marche region was not in the instrumental catalog we used, the hazard results give considerable PGA values for the whole region. The expected PGA values using background seismic-source models reflect the distribution of the instrumental seismicity of the past two decades (CSTI catalog, Fig. 2), with some important peculiarities. For example, the seismicity concentrated in the volcanic district of Lake Bolsena (northwest of Viterbo) has a minimum impact on the hazard maps, whereas a few events concentrated in the Lake Trasimeno (west of Perugia) zone give relatively high hazard, which follows westward (on the boundary of our maps) because of the contribution of the Tuscan seismicity (M. Amiata seismicity). Finally, the area around the town of Chieti, affected, on the whole, by only few events in the 1981–1996 period, gives a relative maximum, with expected PGA values between $0.20g$ and $0.25g$.

These PGA levels are significant in terms of seismic risk reduction, even if they derive from low-level seismicity, always neglected by Italian PSH studies in the past. Notably, the background hazard map has spatial variations, following the *a* and *b* coefficient fluctuations, a feature unlikely to happen when using extended areal sources (SPs).

Flat, low, and spatially homogeneous PGA values result despite the use of the seismotectonic provinces (G-R models of SPs A, C, and D in Fig. 7); by spreading the available seismicity over the whole area, the hazard is considerably reduced, with PGA values as high as $0.10g$ (Fig. 10b). Only the influence of the nearby individual SBs make them higher (0.10–$0.20g$). Inside SP B, in Figure 10b, the distribution of hazard is strictly correlated to the location and the geometry of the individual SBs. The partial overlap of sources, due to the 3D geometry, creates one spot of PGA values ($>0.40g$). Moreover, the choices on the energetic parameterization of the SBs made important differences to the expected PGA values; in fact, the SBs modeled with an exclusive "characteristic earthquake" model have less impact than those with a G-R behavior, both with pure G-R distribution (e.g., SBs 4, 7, 16, 17, and 24) or with a Hybrid model (e.g., SBs 8, 9, and 20). In addition, the expected PGA is larger when the source fault is relatively short (e.g., SBs 7 and 12), because the smaller maximum magnitude gets shorter recurrences to

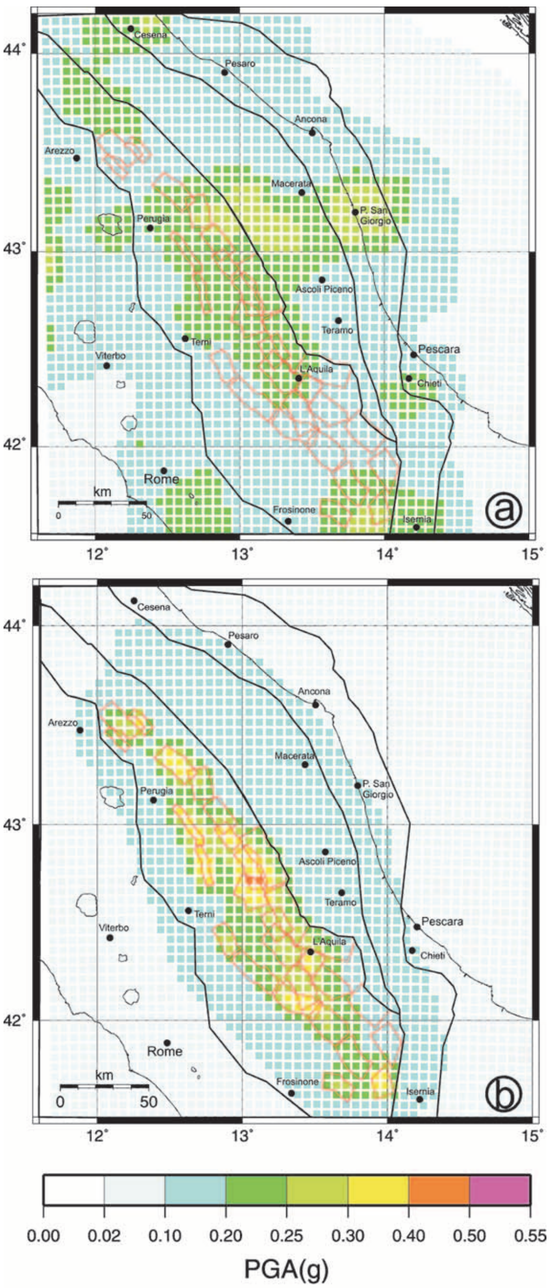

Figure 10. Maps of PGA expected not to be exceeded in 50 years at 90% probability level in central Italy, with standard deviation in attenuation (Ambraseys *et al.*, 1996), using the low-level background seismicity modeling (a) and the models of the seismotectonic provinces and of the seismogenic boxes (b).

a given slip rate, producing high hazard. For longer faults (e.g., SBs 1, 2, 3, and 19), although the recurrence rates are low, they may dominate longer return-period ground motions because of the larger maximum magnitudes.

The final poissonian results (Fig. 11) were obtained using all the source models. On average, the PGA values are higher than those obtained with traditional models (e.g., Slejko *et al.*, 1998; Gruppo di Lavoro, 1999; Romeo *et al.*, 2000; Albarello *et al.*, 2000; Lucantoni *et al.*, 2001; Gruppo

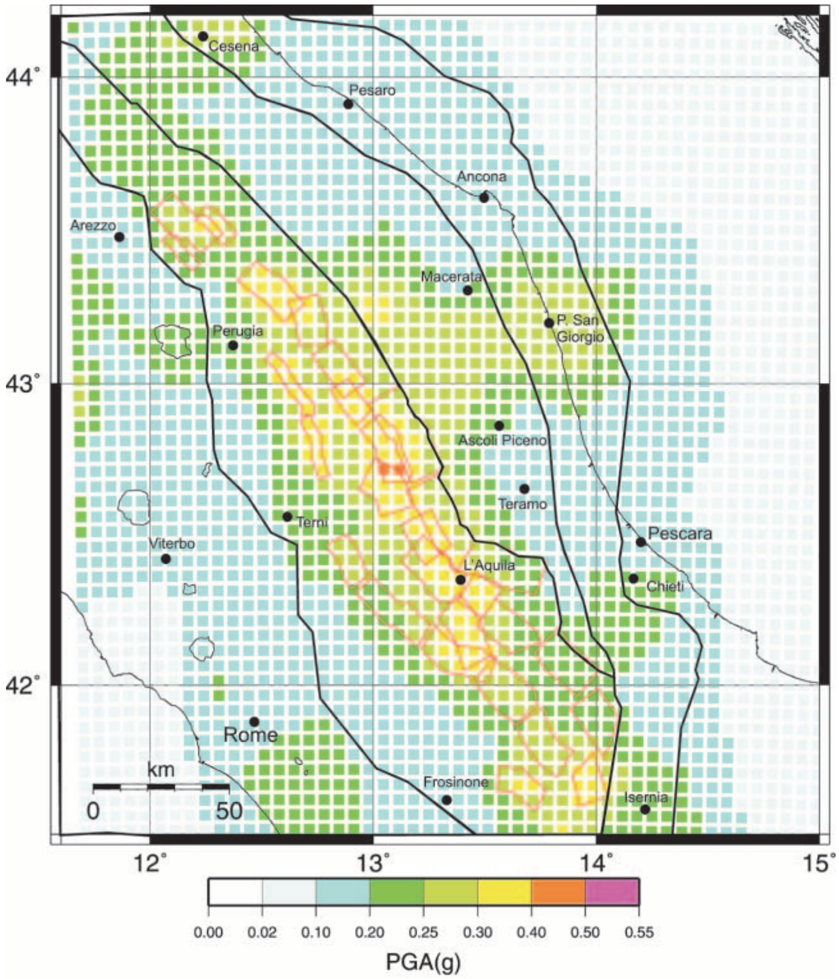

Figure 11. Map of PGA expected not to be exceeded in 50 years at 90% probability level in central Italy, with standard deviation in attenuation (Ambraseys *et al.*, 1996), using the layered-source model.

di Lavoro, 2004); the influence of the individual sources and the background seismicity model is clear. The most recent national seismic hazard map (Gruppo di Lavoro, 2004) gives maximum values of PGA between $0.25g$ and $0.275g$, located on the southern part of the axial Apennine chain studied here. In the same area, our maps give values that can be 50% higher, with localized spikes with values at about $0.4g$. Our maps are more variable, following the individual sources pattern and the fluctuations modeled by the background seismicity; we identify areas with relatively high hazard outside the axial SP B too, with PGA values $>0.25g$ (e.g., P. San Giorgio area) despite the values between 0.175 and $0.2g$ of the national map. The volcanic areas (e.g., Colli Albani area, south of Rome), clearly visible in both the maps, again reach higher values in our maps (0.2–$0.25g$ versus 0.15–$0.175g$); in our analysis they are not connected to the axial belt of maximum hazard but concentrated only in the volcanic districts. Their shapes follow the lateral variation of the seismicity only and are not forced by the zoning. Finally, our maps are little influenced by the geometry of the seismotectonic provinces, which can be considered equivalent in their meaning to the "seismogenic zones" used in the Gruppo di Lavoro (2004) model.

The Time-dependent Hazard Assessment

The last goal of our article is to introduce time dependence into the seismic-hazard analysis. We chose to produce maps in which the time elapsed since the last maximum event, when known, entered into the computations. We therefore adopted the simplest time-dependent process, namely the renewal one. The time dependency has been associated with the seismogenic boxes only, using the formulation of Brownian passage-time (BPT) distributions, one of the most physically motivated models that has appeared in recent literature (Matthews *et al.*, 2002). The time-dependent model is only applicable to the individual sources, because only for these sources do we know or we infer the date of the last maximum earthquake (see Fig. 4 and Table 2).

The time elapsed since the last event is used to determine the conditional probability of having an event in the next 50 years. Input parameters for the calculation of the probability of occurrence of an earthquake for an individual source are: T_{ela}, the time elapsed since the most recent maximum earthquake; μ, the mean recurrence time; and α, a dimensionless measure of aperiodicity given by (see Matthews *et al.* [2002] for details):

$$\alpha = \sqrt{\frac{\text{variance}}{\text{Tmean}}} \tag{6}$$

The conditional probability of an earthquake not having occurred prior to T_{ela} can be calculated from these equations:

$$P(t \leq T \leq t + \Delta T) = \int_{t}^{t+\Delta T} \left(\frac{\mu}{2\pi\alpha^2 u^3}\right)^{1/2} \exp\left(-\frac{(u-\mu)^2}{2\alpha^2 \mu u}\right) du \tag{7}$$

$$P(Te \leq T \leq Te + \Delta T/T > Te) = \frac{P(Te \leq T \leq Te + \Delta T)}{1 - P(0 \leq T \leq Te)} \tag{8}$$

Because we do not have experimental data of repeated earthquakes on the individual structures we decided to use the statistics on the calculated $T_{M_{max}}$ to derive μ and α values (Fig. 5 and Table 3). For sources without a dated major event (see Table 2, source code underlined in Fig. 12) we imposed 4000 years of elapsed time, taking into consideration the completeness stated by historical and archeological studies in central Italy (e.g., Guidoboni and Mariotti, 1997; Stucchi and Albini, 2000; Galadini and Galli, 2001) for the highest level of energy; however, these sources will be treated in the following discussions under Poisson assumptions.

Figure 12 compares the mean recurrence times with the time that elapsed since the last maximum event and gives the BPT conditional probabilities for the next 50 years. From the graph we recognize that less than 50% of the sources exhibit an appreciable probability value in the next 50 years (2004–2053). Among them, some sources like SBs 12, 13, 15, 21, and 28 have a $T_{ela} \approx \mu$; sources 14, 19, 20, 23, and 24 have an elapsed time two to three times longer than the mean recurrence time and an α value $\approx$ 1/4. These are, with SB 21, the sources most prone to a maximum event in the future, according to these analyses. Significant values of conditional probability are also associated with recently activated sources, such as SBs 26 and 27, because of the high α value. Finally, when the T_{ela} is greater than 3 μ, usually, the conditional probability drops, due to the regular seismic cycle modeled by small (<0.3) α values.

Then, using the simplification proposed by Wu *et al.* (1995), equivalent fictitious seismicity rates have been merged into the seismic-hazard code; the fictitious recurrence time T_{eq} for the M_{max} is computed by solving the equivalence of the probabilities given by

$$P_{Tdep} = P_{Pois} = 1 - e^{-t/T_{eq}} \tag{9}$$

where P_{Tdep}, the conditional probability obtained by the BPT model (Fig. 12), is set equal to the probability of a Poisson process, given a selected observation period t (here, 50 years). The T_{eq} is then used instead of $T_{M_{max}}$ with the limitations that the analysis can be done only for the selected observation period.

Uncertainties in terms of M_{max} and $T_{M_{max}}$ enter directly into the distribution functions; the uncertainty on the characteristic event is the standard deviation of the Gaussian magnitudes distribution; the aperiodicity α in BPT function represents the uncertainty in the temporal behavior.

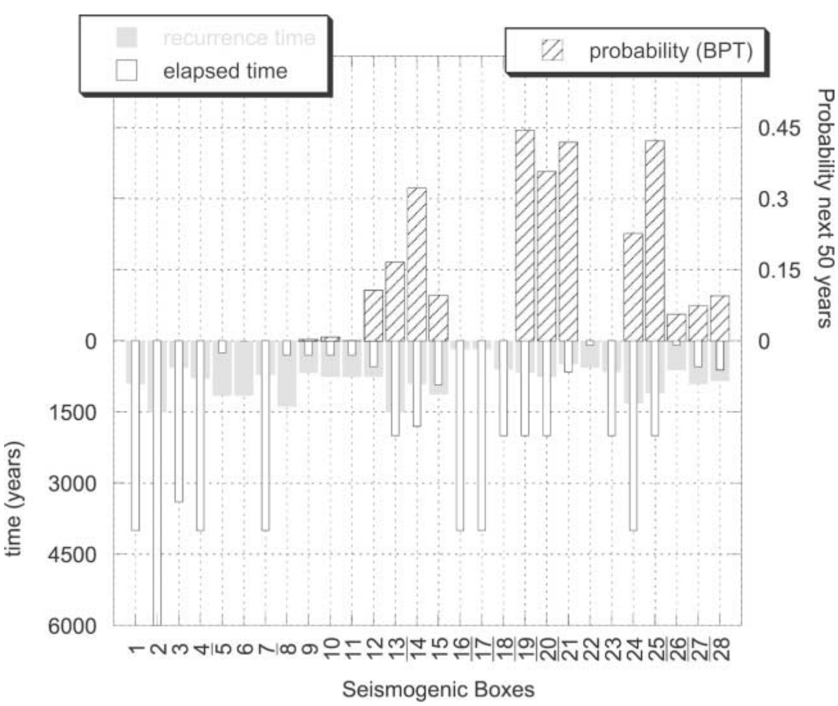

Figure 12. Quantities related to the renewal process adopted for some seismogenic boxes. In the lower part of the graph (axis on the left) mean recurrence time and time elapsed since the last event (known or inferred) are shown. In the upper part (axis on the right), conditional probability of occurrence of a M_{max} event in the next 50 years (from 2004) using BPT distribution is shown.

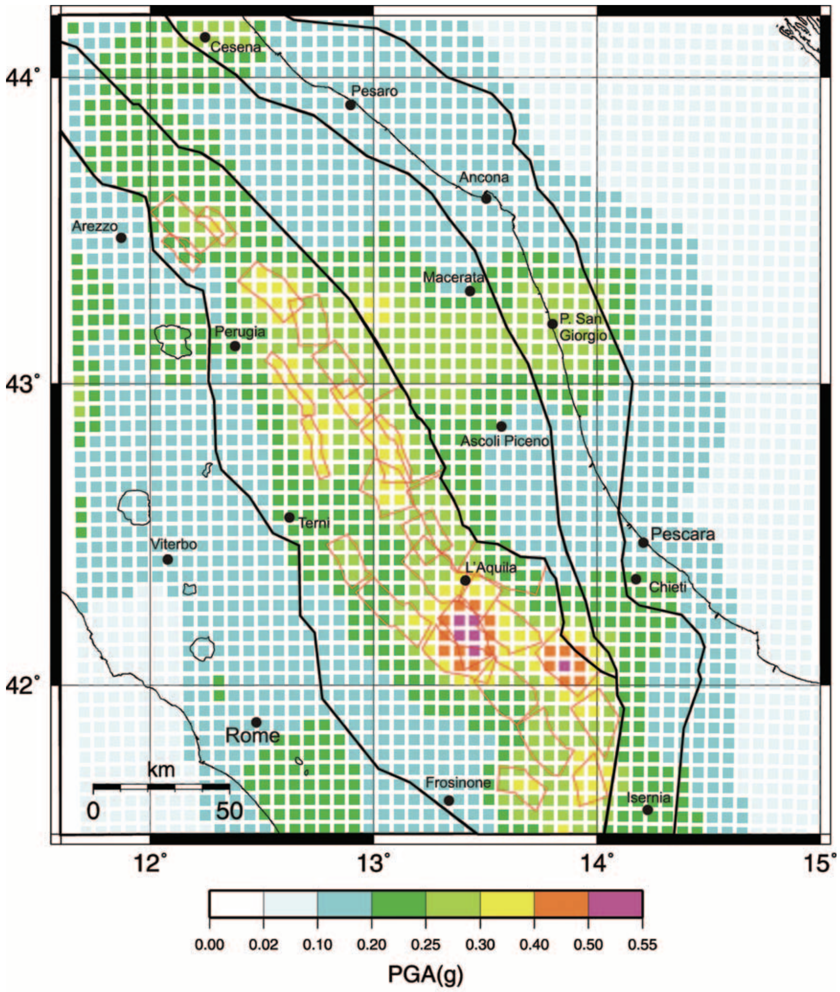

Figure 13. Map of PGA expected not to be exceeded in the next 50 years (from 2004) at 90% probability level in central Italy, with standard deviation in attenuation (Ambraseys *et al.*, 1996), using the layered and time-dependent source model.

The results of the application of the time-dependent model, in terms of expected PGA values in the next 50 years, are illustrated in the seismic hazard map of Figure 13. The picture is quite different from the one obtained under Poisson assumptions. The contribution of the recently active sources, like SB 6 (Colfiorito) or SB 22 (Fucino) (activated during the 1997 and 1915 earthquakes, respectively; Table 2), vanishes in the overall seismic hazard. On the other hand, some sources, for the high BPT conditional probabilities (Fig. 12), become the most hazardous sites (SB 21, Campo Felice-Ovindoli, and SB 14, Sulmona), with PGA values $>0.5g$. The spot with expected PGa $>0.4g$ in the Poissonian map (Fig. 11) are now only as high as $0.3g$; L'Aquila becomes the most hazardous city in the study area as a consequence of the probable activity on the southernmost structure of Campo Felice-Ovindoli (SB 21) in the time-dependent model. The differences between stationary and nonstationary maps are illustrated in Figure 14; in the area where we have an increasing of hazard in the time-dependent map (area between Campo Felice-Ovindoli and Sulmona), the PGA values are about 50% higher (Fig. 14a) than the Poissonian ones, with a maximum increase up to $0.25g$ (Fig. 14b); on the contrary, in the areas where the nonstationary results decrease with respect to the stationary ones (e.g., the Umbria-Marche area and the Fucino area), the values are locally up to 20% lower (Fig. 14 a) with a maximum decrease of about $0.07g$ (Fig. 14 b).

Final Remarks

We have developed a new seismogenic source model with the relative seismic-hazard maps for central Italy. The methodology can be considered an attempt to use all the available seismological, geological, and geophysical information of an active area to obtain probabilistic evaluation of the expected ground shaking. In the area studied numerous detailed geological and geophysical data are available together with good records of paleohistorical and instrumental earthquakes.

The elaborated model is a layered model, where the available information enters at different levels into the seismic-hazard computation. The individual structures liable to undergo major earthquakes ($M \geq 5.5$) are parameterized in terms of "seismogenic box," representing the plan projection

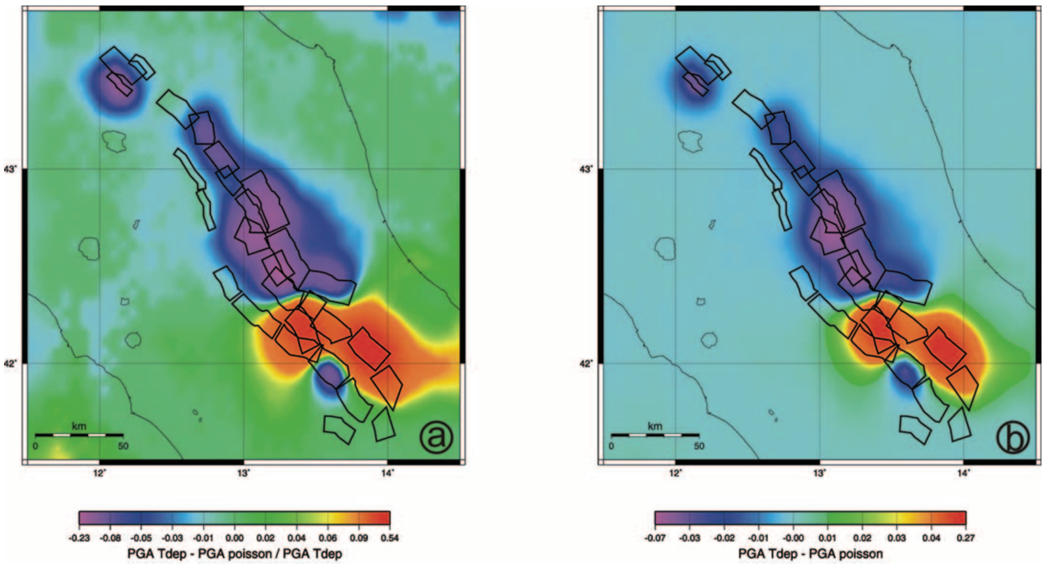

Figure 14. Comparison of Poisson (see Fig. 11) and time-dependent (see Fig. 13) results: (a) relative differences expressed in percentage of PGA; (b) absolute differences in g.

of active faults; the magnitude (M) and recurrence time (T) distributions are calibrated independently on the geometric and kinematic constraints and by the earthquake-structure association; they are also adequate for use in a time-dependent approach. The background seismicity (M approximately <5.5) is evaluated using the instrumental seismicity registered in the past two decades. The remaining seismicity is modeled with seismotectonic provinces that are defined using geological-structural and seismotectonic information. The global seismogenic source model proposed here represents seismic-moment release conditions compatible with the long-lasting series of seismological observations and with the few geodetic data available for the area.

The seismic-hazard computations use both Poisson and non-Poisson hypotheses. In addition to the common stationary assumptions, a time-dependent hypothesis has been introduced; by adopting equivalent fictitious seismicity rates, starting from conditional probabilities computed by BPT distributions, we obtain maps referring to the next 50 years (from 2004 onward) by using public traditional codes, with an accuracy that is acceptable for engineering purposes.

Some questions still remain, like the evaluation of the uncertainties introduced in the model, or the definition of new individual sources. Nevertheless, we believe that the PSH assessments presented here represent, in actual fact, the most complete regional evaluations in terms of complexity and use of all the available data. The reduction of the critical uncertainties (e.g., slip rates and recurrence times) needs additional studies aimed, in particular, at evaluating all the geological markers.

We consider the methodology and results obtained useful for the strategies of seismic risk reduction.

Acknowledgments

This study was supported by M.I.U.R. grants to G. Lavecchia (COFIN 2004 prot. 2004044512) and by INGV-GNDT funds to L. Peruzza (Project "Terremoti probabili in Italia tra l'anno 2000 e il 2030: elementi per la definizione di priorità degli interventi di riduzione del rischio sismico" coordinated by A. Amato and G. Selvaggi). We thank the two anonymous reviewers and Editor Andy Michael for their valuable comments on the manuscript.

References

Aki, K. (1965). Maximum likelihood estimate of b in the formula logN = a-bM and its confidence limits, *Bull. Earthquake Res. Inst.* **43,** 237–239.

Albarello, D., V. Bosi, F. Bramerini, A. Lucantoni, G. Naso, L. Peruzza, A. Rebez, F. Sabetta, and D. Slejko (2000). Carte di pericolosità sismica del territorio nazionale, *Quad. Geofis.* **12,** 7 pp.

Amato, A., R. Azzara, C. Chiarabba, G. B. Cimini, M. Cocco, M. Di Bona, L. Margheriti, S. Mazza, F. Mele, G. Selvaggi, A. Basili, E. Boschi, F. Courboulex, A. Deschamps, S. Gaffet, G. Bittarelli, L. Chiaraluce, D. Piccinini, and M. Ripepe (1998). The 1997 Umbria-Marche, Italy, earthquake sequence: a first look at the main shocks and aftershocks, *Geophys. Res. Lett.* **25,** 2861–2864.

Amato, A., and G. Selvaggi (2004). Probable earthquakes in Italy from year 2000 to 2030: guidelines for determining priorities in seismic risk mitigation, Gruppo Nazionale per la Difesa dai Terremoti, Brief Report, 34 pp., http://gndt.ingv.it/Att_scient/PE2002_Brief_Reports/brief_reports.htm (last accessed July 2005).

Ambraseys, N. N., K. A. Simpson, and J. J. Bommer (1996). Prediction of horizontal response spectra in Europe, *Earthquake Eng. Struct. Dyn.* **25,** 371–400.

Amoruso, A., L. Crescentini, and R. Scarpa (1998). Inversion of source parameters from near- and far-field observations: an application to the 1915 Fucino earthquake, central Apennines, Italy, *J. Geophys. Res.* **103,** 29,989–29,999.

Argnani, A., G. Barbacini, M. Bernini, F. Camurri, M. Ghielmi, G. Papani,

F. Rizzini, S. Rogledi, and L. Torelli (2003). Gravity tectonics driven by Quaternary uplift in the northern Apennines: insights from the La Spezia-Reggio Emilia geo-transect, *Quat. Int.* **101–102,** 13–26.

Argnani, A., M. Bernini, G. M. Di Dio, G. Papani, and S. Rogledi (1997). Stratigraphic record of crustal-scale tectonics in the Quaternary of northern Apennines (Italy), *Il Quaternario* **10,** 595–602.

Baratta, M. (1901). I terremoti d'Italia. Saggio di storia geografia e bibliografia sismica italiana, Torino, 951 pp.

Barchi, M., F. Galadini, G. Lavecchia, P. Messina, A. M. Michetti, L. Peruzza, A. Pizzi, E. Tondi, and E. Vittori (Editors) (2000). *Sintesi delle conoscenze sulle faglie attive in Italia Centrale: parametrizzazione ai fini della carattrizzazione della pericolosità sismica*, CNR-GNDT, Rome, 62 pp.

Bender, B., and D. M. Perkins (1987). SEISRISK III; a computer program for seismic hazard estimation, U.S. Geological Survey, Reston, Virginia, 48 pp.

Blumetti, A. M. (1995). Neotectonic investigations and evidence of paleoseismicity in the epicentral area of the January-February 1703, central Italy, earthquakes, *Perspect. Paleoseism.* **6,** 83–100.

Boatwright, J., H. Bundock, J. Luetgert, L. Seekins, I. Gee, and P. Lombard (2003). The dependence of PGA and PGV on distance and magnitude inferred from Northern California ShakeMap data, *Bull. Seism. Soc. Am.* **93,** 2043–2055.

Boncio, P., F. Brozzetti, and G. Lavecchia (2000). Architecture and seismotectonics of a regional low-angle normal fault zone in central Italy, *Tectonics* **19,** 1038–1055.

Boncio, P., and G. Lavecchia (2000a). A structural model for active extension in Central Italy, *J. Geodyn.* **29,** 233–244.

Boncio, P., and G. Lavecchia (2000b). A geological model for the Colfiorito earthquakes (September-October 1997, Central Italy), *J. Seism.* **4,** 345–356.

Boncio, P., G. Lavecchia, and B. Pace (2004a). Defining a model of 3D seismogenic sources for Seismic Hazard Assessment applications: the case of central Apennines (Italy), *J. Seism.* **8,** 407–425.

Boncio, P., G. Lavecchia, G. Milana, and B. Rozzi (2004b). Improving the knowledge on the seismogenesis of the Amatrice-Campotosto area (central Italy) through an integrated analysis of minor earthquake sequences and structural data, *Ann. Geophys.* **47,** 1723–1742.

Boschi, E., G. Ferrari, P. Gasperini, E. Guidoboni, G. Smriglio, and G. Valensise (1995). *Catalogo dei forti terremoti in Italia dal 461 a.C. al 1980*, ING-SGA, Bologna, 973 pp.

Boschi, E., E. Guidoboni, G. Ferrari, G. Valensise, and P. Gasperini (1997). *Catalogo dei forti terremoti in Italia dal 461 a.C. al 1990, No. 2*, ING-SGA, Bologna, 644 pp.

Bragato, P. L. (2004). Regression analysis with truncated samples and its application to ground-motion attenuation studies, *Bull. Seism. Soc. Am.* **94,** 1369–1378.

Brozzetti, F., P. Boncio, and G. Lavecchia (2001). A new interpretation of the CROP 03 seismic profile across the northern Tiber Valley and inferences about the seismotectonics of the Città di Castello–Sansepolcro area, Geoitalia 2001, Volume dei Riassunti, 337–338.

Camassi, R., and M. Stucchi (1997). *NT 4.1: un catalogo parametrico di terremoti di area italiana al di sopra della soglia del danno*, CNR-GNDT Milano, 95 pp., http://emidius.itim.mi.cnr.it/NT.html (last accessed July 2005).

Castello, B., G. Selvaggi, C. Chiarabba, and A. Amato (2005). CSI Catalogo della sismicità italiana 1981–2002, vers. 1.0, INGV-CNT, Roma, www.ingv.it/CSI/ (last accessed July 2005).

Cattaneo, M., P. Augliera, G. De Luca, A. Gorini, A. Govoni, S. Marcucci, A. Michelini, G. Monachesi, D. Spallarossa, and L. Trojani, and eXperimental Group for Umbria-Marche Seismicity (2000). The 1997 Umbria-Marche (Italy) earthquake sequence: analysis of the data recorded by the local and temporary networks, *J. Seism.* **4,** 401–414.

Cello, G., G. Deiana, P. Mangano, S. Mazzoli, E. Tondi, L. Ferreli, L. Maschio, A. M. Michetti, L. Serva, and E. Vittori (1998). Evidence for surface faulting during the September 26, 1997, Colfiorito (Central Italy) earthquakes, *J. Earthquake Eng.* **2,** 303–324.

Cinti, F. R., L. Cucci, F. Marra, and P. Montone (2000). The 1997 Umbria-Marche earthquakes (Italy): relations between the surface tectonic breaks and the area of deformation, *J. Seism.* **4,** 333–343.

D'Addezio, G., E. Masana, and D. Pantosti (2001). The Holocene paleoseismicity of the Aremogna-Cinque Miglia fault (central Italy), *J. Seism.* **5,** 181–205.

Decandia, F. A., A. Lazzarotto, D. Liotta, L. Cernobori, and R. Nicolich (1998). The CROP 03 traverse: insights on postcollisional evolution of the Northern Apennines. *Mem. Soc. Geol. Ital.* **52,** 427–439.

Di Luccio, F., A. Amato, R. M. Azzara, A. Basili, A. Della dio, M. Di Bona, A. Gorini, F. P. Lucente, S. Marcucci, L. Margheriti, G. Milana, F. Ponziani, G. Selvaggi, and E. Zambonelli (1997). La sequenza sismica del maggio 1997 a Massa Martana (PG), 16° Convegno GNGTS, Roma, 11–13 novembre 1997, Riassunti delle comunicazioni, 65.

Douglas, J. (2003). Earthquake ground motion estimation using strong-motion records: a review of equations for the estimation of peak ground acceleration and response spectral ordinates, *Earth Sci. Rev.* **61,** 43–104.

Ekström, G., and A. M. Dziewonski (1988). Evidence of bias in the estimation of earthquake size, *Nature* **332,** 319–323.

Faenza, L., W. Marzocchi, and E. Boschi (2003). A non-parametric hazard model to characterize the spatio-temporal occurrence of large earthquakes; an application to the Italian catalogue, *Geophys. J. Int.* **155,** 521–531.

Field, E. H., D. D. Johnson, and J. F. Dolan (1999). A mutually consistent seismic-hazard source model for Southern California, *Bull. Seism. Soc. Am.* **89,** 559–678.

Field, E. H., T. H. Jordan, and C. A. Cornell (2003). OpenSHA: a developing community-modeling environment for seismic hazard analysis, *Seism. Res. Lett.* **74,** 406–419.

Frankel, A. (1995). Mapping seismic hazard in the central and eastern United States, *Seism. Res. Lett.* **66,** 8–21.

Frankel, A. D., M. D. Petersen, C. S. Mueller, K. M. Haller, R. L. Wheeler, E. V. Leyendecker, R. L. Wesson, S. C. Harmsen, C. H. Cramer, D. M. Perkins, and K. S. Rukstales (2002). Documentation for the 2002 update of the national seismic hazard maps, *U.S. Geol. Surv. Open-File Rept 02-420*.

Frepoli, A., and A. Amato (1997). Contemporaneous extension and compression in the Northern Apennines from earthquake fault-plane solutions, *Geophys. J. Int.* **129,** 368–388.

Frezzotti, M., and C. Giraudi (1989). Evoluzione geologica tardo-pleistocenica ed olocenica del Piano di Aremogna (Roccaraso-Abruzzo): implicazioni climatiche e tettoniche, *Mem. Soc. Geol. Ital.* **42,** 5–19.

Galadini, F., and P. Galli (1999). The Holocene paleoearthquakes on the 1915 Avezzano earthquake faults (central Italy); implications for active tectonics in the central Apennines, *Tectonophysics* **308,** 143–170.

Galadini, F., and P. Galli (2000). Active tectonics in the Central Apennines (Italy)—input data for seismic hazard assessment, *Nat. Hazards* **22,** 225–270.

Galadini, F., and P. Galli (2001). Archaeoseismology in Italy: case studies and implications on long-term seismicity, *J. Earthquake Eng.* **5,** 35–68.

Galadini, F., and P. Galli (2003). Paleoseismology of silent faults in the Central Apennines (Italy): the Mt. Vettore and Laga Mts. faults, *Ann. Geophys.* **5,** 815–836.

Galadini, F., P. Galli, and C. Giraudi (1997a). Paleosismologia della Piana del Fucino (Italia centrale), *Il Quaternario* **10,** 27–64.

Galadini, F., P. Galli, and C. Giraudi (1997b). Geological investigations of italian earthquakes: new paleoseismological data from the Fucino plain (central Italy), *J. Geodyn.* **24,** 87–103.

Galadini, F., P. Galli, and M. Moro (2003). Paleoseismology of silent faults in the Central Apennines (Italy): the Campo Imperatore fault (Gran Sasso Range Fault System), *Ann. Geophys.* **5,** 793–813.

Galadini, F., C. Meletti, and E. Vittori (2000). Stato delle conoscenze sulle faglie attive in Italia: elementi geologici di superficie, in *Le ricerche del GNDT nel campo della pericolosità sismica (1996–1999)*, F. Galadini, C. Meletti, and A. Rebez (Editors), CNR-GNDT, Rome, 107–136.

Gardner, J. K., and L. Knopoff (1974). Is the sequence of earthquakes in southern California, with aftershocks removed, Poissonian?, *Bull. Seism. Soc. Am.* **64,** 1363–1367.

Gasparini, C., G. Iannaccone, and R. Scarpa (1985). Fault-plane solutions and seismicity of the Italian peninsula, *Tectonophysics* **117,** 59–78.

Gasperini, P., F. Bernardini, G. Valensise, and E. Boschi (1999). Defining seismogenic sources from historical earthquake felt reports, *Bull. Seism. Soc. Am.* **89,** 94–110.

Giraudi, C., and M. Frezzotti (1995). Paleoseismicity in the Gran Sasso massif (Abruzzo, Central Italy), *Quat. Int.* **25,** 81–93.

Gruppo di Lavoro (1999). Proposta di riclassificazione sismica del territorio nazionale, *Ingegneria Sismica* **16,** no. 1, 5–14.

Gruppo di Lavoro (2004). *Redazione della mappa di pericolosità sismica prevista dall'Ordinanza PCM 3274 del 30 marzo 2003*, Rapporto conclusivo per il Dipartimento di Protezione Civile, INGV, Milano-Roma, 65 pp.

Guidoboni, E., and D. Mariotti (1997). I terremoti "sconosciuti": appunti per un catalogo, in *Catalogo dei forti terremoti in Italia dal 461 a.C. al 1990*, no. 2, E. Boschi, E. Guidoboni, G. Ferrari, G. Valensise, and P. Gasperini (Editors), ING-SGA, Roma-Bologna, 80–90.

Gutenberg, B., and C. F. Richter (1944). Frequency of earthquakes in California, *Bull. Seism. Soc. Am.* **34,** 185–188.

Hanks, T. C., and H. Kanamori (1979). A moment magnitude scale, *J. Geophys. Res.* **84,** 2348–2350.

Hunstad, I., G. Selvaggi, N. D'Agostino, P. England, P. Clarke, and M. Pierozzi (2003). Geodetic strain in peninsular Italy between 1875 and 2001, *Geophys. Res. Lett.* **4,** 1181–1186.

Knopoff, L. (2000). The magnitude distribution of declustered earthquakes in Southern California, *Proc. Natl. Acad. Sci. USA* **97,** 11,880–11,884.

Knopoff, L., Y. Y. Kagan, and R. Knopoff (1982). b-values for foreshocks and aftershocks in real and simulated earthquake sequences, *Bull. Seism. Soc. Am.* **72,** 1663–1679.

Lavecchia, G., P. Boncio, F. Brozzetti, M. Stucchi, and I. Leschiutta (2002). New criteria for seismotectonic zoning in central Italy: insights from the Umbria-Marche Apennines, *Boll. Soc. Geol. Ital.*, vol. sp. 1-2002, 881–890.

Lavecchia, G., P. Boncio, and N. Creati (2003). A lithospheric-scale seismogenic thrust in central Italy, *J. Geodyn.* **36,** 79–94.

Lavecchia, G., F. Brozzetti, M. Barchi, J. Keller, and M. Menichetti (1994). Seismotectonic zoning in east-central Italy deduced from the analysis of the Neogene to present deformations and related stress fields, *Soc. Geol. Am. Bull.* **106,** 1107–1120.

Lolli, B., and P. Gasperini (2003). Aftershocks hazard in Italy. Part I: Estimation of time-magnitude distribution model parameters and computation of probabilities of occurrence, *J. Seism.* **7,** 235–257.

Lucantoni, A., V. Bosi, F. Bramerini, R. De Marco, T. Lo Presti, G. Naso, and F. Sabetta (2001). Il rischio sismico in Italia, *Ingegneria Sismica* **1,** 5–36.

Margottini, C., N. N. Ambraseys, and A. Screpanti (1993). *La magnitudo dei terremoti italiani del XX secolo*, ente per le nuove tecnologie, l'energide l'ambiente, Roma, 57 pp.

Marzocchi, W., L. Sandri, and E. Boschi (2003). On a validation of earthquake-forecasting models: the case of pattern recognition algorithms, *Bull. Seism. Soc. Am.* **93,** 1994–2004.

Matthews, M. V., W. L. Ellsworth, and P. A. Reasenberg (2002). A Brownian model for recurrent earthquakes, *Bull. Seism. Soc. Am.* **92,** 2233–2250.

Meletti, C., E. Patacca, and P. Scandone (2000). Construction of a seismotectonic model: the case of Italy, *Pure Appl. Geoph.* **157,** 11–35.

Michetti, A. M., F. Brunamonte, L. Serva, and E. Vittori (1996). Trench investigations of the 1915 Fucino earthquake fault scarps (Abruzzo, central Italy): geological evidence of large historical events, *J. Geophys. Res.* **101,** 5921–5936.

Michetti, A. M., F. Brunamonte, L. Serva, and R. A. Whitney (1995). Seismic hazard assessment from paleoseismological evidence in the Rieti Region, Central Italy, *Perspec. Paleoseism.* **6,** 63–82.

Monachesi, G., and M. Stucchi (Editors) (1997). DOM 4. 1: an intensity database of damaging earthquakes in the Italian area, http://emidius.mi.ingv.it/DOM (last accessed July 2005).

Montone, P., A. Amato, and S. Pondrelli (1999). Active stress map of Italy, *J. Geophys. Res.* **104,** 25,595–25,610.

Morewood, N. C., and G. P. Roberts (2000). The geometry, kinematics and rates of deformation within an en échelon normal fault segment boundary, central Italy, *J. Struct. Geol.* **22,** 1027–1047.

Oddone, E. (1915). Gli elementi fisici del grande terremoto Marsicano-Fucense del 13 Gennaio 1915, *Boll. Soc. Sism. Ital.* **19,** 71–216.

Pace, B., P. Boncio, and G. Lavecchia (2002a). The 1984 Abruzzo earthquake (Italy): an example of seismogenic process controlled by interaction between differently-oriented sinkinematic faults, *Tectonophysics* **350,** 237–254.

Pace, B., L. Peruzza, G. Lavecchia, and P. Boncio (2002b). Seismogenic sources in Central Italy: from causes to effects, *Mem. Soc. Geol. Ital.* **57,** 419–429.

Pantosti, D., G. D'Addezio, and F. R. Cinti (1996). Paleoseismicity of the Ovindoli-Pezza fault, central Apennines, Italy: a history including a large, previously unrecorded earthquake in the Middle ages (860–1300 A.D.), *J. Geophys. Res.* **101,** 5937–5959.

Parolai, S., L. Trojani, G. Monachesi, M. Frapiccini, M. Cattaneo, and P. Augliera (2001). Hypocenter location accuracy and seismicity distribution in the Central Apennines (Italy), *J. Seism.* **5,** 243–261.

Peruzza, L. (Editor) (1999). *Progetto MISHA Metodi Innovativi per la Stima dell'HAzard: applicazione all'Italia Centrale*, CNR-GNDT, Trieste, 176 pp.

Peruzza, L., and B. Pace (2002). Sensitivity analysis for seismic source characteristics to probabilistic seismic hazard assessment in central Apennines (Abruzzo area), *Boll. Geofis. Teor. Appl.* **43,** 79–100.

Peruzza, L., D. Pantosti, D. Slejko, and G. Valensise (1997). Testing a new hybrid approach to seismic hazard assessment: an application to the Calabrian Arc (Southern Italy), *Nat. Hazards* **14,** 113–126.

Pialli, G., M. R. Barchi, and G. Minelli (Editor) (1998). Results of the CROP 03 deep seismic reflection profile, *Mem. Soc. Geol. Ital.* **52,** 657 pp.

Reasenberg, P. A. (1985). Second-order moment of central California seismicity, 1969–1982, *J. Geophys. Res.* **90,** 5479–5495.

Reasenberg, P. A., and L. M. Jones (1989). Earthquake hazard after a mainshock in California, *Science* **243,** 1173–1176.

Reasenberg, P. A., and L. M. Jones (1994). Earthquake aftershocks: update, *Science* **265,** 1251–1252.

Riguzzi, F., A. Tertulliani, and C. Gasparini (1989). Study of the seismic sequence of Porto San Giorgio (Marche), 3 July 1987, *II Nuovo Cimento* **12,** 453–467.

Romeo, R. (2005). Earthquake hazard in Italy, 2001–2030, *Nat. Hazards* **36,** 383–405.

Romeo, A., A. Paciello, and D. Rinaldis (2000). Seismic hazard maps of Italy including site effects, *Soil Dyn. Earthquake Eng.* **20,** 85–92.

Salvi, S., F. R. Cinti, L. Colini, G. D'Addezio, F. Doumaz, and E. Pettinelli (2003). Investigation of the active Celano-L'Aquila fault system, Abruzzi (central Apennines, Italy) with combined ground-penetrating radar and paleoseismic trenching, *Geophys. J. Int.* **155,** 805–818.

Santini, S. (2003). A note on Northern Marche seismicity: new focal mechanisms and seismological evidence, *Ann. Geophys.* **46,** 725–731.

Scandone, P., and M. Stucchi (2000). La zonazione sismogenetica ZS4 come strumento per le ricerche GNDT nel campo della pericolosità sismica, in *Le ricerche del GNDT nel campo della pericolosità sismica (1996–1999)*, F. Galadini, C. Meletti, and A. Rebez (Editors), CNR-GNDT, Rome, 3–14.

Scholz, C. H. (1990). *The Mechanics of Earthquakes and Faulting*, Cambridge University Press, Cambridge, 439 pp.

Schwartz, D. P., and K. J. Coppersmith (1984). Fault behavior and characteristic earthquakes: examples from the Wasatch and San Andreas Fault Zones, *J. Geophys. Res.* **89,** 5681–5698.

Selvaggi, G. (1998). Spatial distribution of horizontal seismic strain in the Apennines from historical earthquakes, *Ann. Geofis.* **41,** 241–251.

Selvaggi, G., A. Deschamps, M. Ripepe, and B. Castello (2002). Waveforms, arrival times and locations of the 1997 Colfiorito (Umbria-Marche, Central Italy) aftershocks sequence, *Quad. Geofis.* **21,** 6 CD-ROMs.

Slejko, D., L. Peruzza, and A. Rebez (1998). Seismic hazard maps of Italy, *Ann. Geofis.* **41,** 183–214.

Slejko, D., and A. Rebez (2002). Probabilistic seismic hazard assessment and deterministic ground shaking scenarios for Vittorio Veneto (N.E. Italy), *Boll. Geofis. Teor. Appl.* **43,** 263–280.

Stirling, M. W., G. H. McVerry, and K. R. Berryman (2002). A new seismic hazard model for New Zealand, *Bull. Seism. Soc. Am.* **92,** 1878–1903.

Stucchi, M. (1985). The earthquakes in central Italy, January-February 1703. Some questions, some preliminary answers, in Atlas of isoseismal maps of Italian earthquakes, D. Postpischl (Editor), *Quad. Ric. Sci.* **114/2A,** 56–57.

Stucchi, M., and P. Albini (2000). Quanti terremoti distruttivi abbiamo perso nell'ultimo millennio? Spunti per la definizione di un approccio storico alla valutazione della completezza, in *Le ricerche del GNDT nel campo della pericolosità sismica (1996–1999)*, F. Galadini, C. Meletti, and A. Rebez (Editors), CNR-GNDT, Rome, 333–343.

Utsu, T. (1965). A method for determining the value of b in the formula logN = a-bM showing the magnitude-frequency relation for earthquakes, *Geophys. Bull. Hokkaido Univ.* **13,** 99–103.

Utsu, T. (1966). A statistical significance test of the difference in b-value between two earthquake groups, *J. Phys. Earth* **14,** 37–40.

Valensise, G., and D. Pantosti (Editors) (2001). Database of potential sources for earthquakes larger than M 5.5 in Italy, *Ann. Geofis.* **44** (suppl.), 180 pp., with CD-ROM.

Ward, S. N., and G. R. Valensise (1989). Fault parameters and slip distribution of the 1915 Avezzano, Italy, earthquake derived from geodetic observations, *Bull. Seism. Soc. Am.* **79,** 690–710.

Weichert, D. H. (1980). Estimation of the earthquake recurrence parameters for unequal observation periods for different magnitudes, *Bull. Seism. Soc. Am.* **70,** 1337–1346.

Wells, D. L., and K. J. Coppersmith (1994). New empirical relationships among magnitude, rupture length, rupture width, rupture area, and surface displacement, *Bull. Seism. Soc. Am.* **84,** 974–1002.

WGCEP (Working Group on California Earthquake Probabilities) (1995). Seismic hazards in southern California: probable earthquakes, 1994 to 2024, *Bull. Seism. Soc. Am.* **85,** 379–439.

WGCEP (Working Group on California Earthquake Probabilities) (1999). Earthquake probabilities in the San Francisco Bay Region: 2000 to 2030, *U.S. Geol. Surv. Open-File Rept. 99-517*, http://wrgis.wr.usgs.gov/open-file/of99-517/ (last accessed November 2004).

WGCEP (Working Group on California Earthquake Probabilities) (2003). Earthquake probabilities in the San Francisco Bay Region: 2002 to 2031, *U.S. Geol. Surv. Open-File Rept. 03-214*, http://pubs.usgs.gov/of/2003/of03-214/ (last accessed November 2004).

Working Group CPTI (1999). Catalogo Parametrico dei Terremoti Italiani, ING, GNDT, SGA, SSN (Editors). Bologna, 88 pp., http://emidius.mi.ingv.it/CPTI (last accessed November 2004).

Working Group CPTI (2004). Catalogo Parametrico dei Terremoti Italiani, vers. 2004 (CPT104), INGV Bologna, http://emidius.mi.ingv.it/CPTI (last accessed July 2005).

Working Group CSTI (2001). Catalogo Strumentale dei Terremoti 'Italiani' dal 1981 al 1996, Istituto Nazionale di Geofisica-Gruppo Nazionale per la Difesa dai Terremoti (Editors), vers. 1.0 CD-ROM.

Wu, S. C., C. A. Cornell, and S. R. Winterstein (1995). A hybrid recurrence model and its implication on seismic hazard results, *Bull. Seism. Soc. Am.* **85,** 1–16.

GeoSisLab
Dipartimento di Scienze della Terra
Università degli Studi "G. D'Annunzio"
Via dei Vestini, 30
66013 Chieti Scalo (CH) Italy
b.pace@unich.it
g.lavecchia@unich.it
p.boncio@unich.it
(B.P., G.L., P.B.)

Istituto Nazionale di Oceanografia e di Geofisica Sperimentale (OGS)
Borgo Grotta Gigante 42/c
34010 Sgonico (TS) Italy
lperuzza@inogs.it
(L.P.)

Manuscript received 30 November 2004.